Student thesis series INES nr 352

Estimating and evaluating GPP in the Sahel using MSG/SEVIRI and MODIS satellite data

Gustav Wallner

2015

Department of
Physical Geography and Ecosystem Science
Lund University
Sölvegatan 12
S-223 62 Lund
Sweden

Gustav Wallner (2015). ***Remote sensing of GPP in the Sahel using MSG/SEVIRI and MODIS satellite data***

Master degree thesis, 30 credits in *Physical Geography and Ecosystem Analysis*

Department of Physical Geography and Ecosystem Science, Lund University

Level: Master of Science (MSc)

Course duration: *January* 2015 until *June* 2015

Estimating GPP in the Sahel using MSG/SEVIRI and MODIS satellite data

---

Gustav Wallner

Master thesis, 30 credits, in *Physical Geography and Ecosystem Analysis*

Supervisor: Jonas Ardö
Department of Physical Geography and Ecosystem Science,
Lund University

Exam committee:
Lars Eklundh, Department of Physical Geography and Ecosystem Science
Sadegh Jamali, Department of Physical Geography and Ecosystem Science

ABSTRACT

The aim of this study was to use data from Meteosat Second Generation's Spinning Enhanced Visible and Infrared Imager (MSG/SEVIRI) to calculate the gross primary production (GPP) in the Sahel region of Africa for 2011 and 2012. GPP was calculated using the light use efficiency method, which relates GPP to the absorbed photosynthetically active radiation the light use efficiency. The results were compared with the widely used Moderate Resolution Imaging Spectroradiometer (MODIS) GPP product (MOD17A) and ground measurements using the eddy covariance method, from Dahra, Senegal.

The results show that MSG/SEVIRI derived GPP more accurately represent the *in situ* measurements from the Dahra site compared with MODIS GPP, both for short time changes and the magnitude of GPP. MODIS GPP underestimated the ground measurements during the growing season, findings which were consistent with previous studies of the Sahel. MODIS performed well during the dry season and in replicating the change of seasons.

SVENSK SAMMANFATTNING

Syftet med denna studie var att använda data från Meteosat Second Generation's Spinning Enhanced Visible and Infrared Imager (MSG/SEVIRI) för att beräkna total fotosyntes (GPP) i Sahel-regionen i Afrika för åren 2011 och 2012. GPP beräknades med 'light use efficiecy'-metoden, med vilken man använder den mängd strålning som absorberas av växterna tillsammans med hur effektivt växten använder den för att fixera kol från atmosfären. Resultaten jämfördes med den välanvända MOD17A GPP-datan från Moderate Resolution Imaging Spectroradiometer (MODIS) samt markdata från Dahra i Senegal.

Resultaten visar att GPP beräknat från MSG/SEVIRI-data gav bättre resultat än MODIS-GPP för Dahra, både för korta tidsperioder och för nivåerna av GPP. MODIS GPP underskattade markmätningarna under växtsäsongen, vilket också har observerats av andra studier av Sahel. MODIS GPP var dock bättre under torrsäsongen och för att se årstidsförändringar.

KEYWORDS:

Geography, Physical Geography, GPP, Sahel, Dahra, Remote Sensing, Meteosat, MSG, SEVIRI, MODIS

TABLE OF CONTENTS

1 INTRODUCTION

One of the most important processes in the biosphere is the photosynthetic assimilation of CO_2 from the atmosphere by vegetation. This absorption of carbon is called the gross primary production (GPP). Accurate estimations of GPP on regional to global scale is important for creating accurate climate-carbon cycle models (Beer et al. 2010). GPP can also be used to derive information on how well the biosphere can support humans (Running et al. 2004), as seen in studies such as Abdi et al. (2014) which estimated the supply and demand of carbon needed to support the population with food, feed and fuel. Accurate large-scale estimates of GPP can be an important tool for predicting the risk of future famines and changes in resource availability.

Potential changes in the productivity of the Earth's biosphere is a very important effect of future global change due to a changing climate (Running et al. 2000). Among the continents, Africa is one of the most sensitive to climate change (Niang et al. 2014). The warming of Africa due to climate change is likely to be more than 2^{o} C, with minimum temperatures rising rise faster than maximum temperatures (Niang et al. 2014). Future change in mean annual precipitation (MAP) is uncertain for sub-Saharan Africa, however, the increasing temperatures will exacerbate the already present stress on water availability (Niang et al. 2014).

The Sahel is a region of Africa between the Sahara desert and the savannahs closer to the equator (figure 1). Arid regions such as the Sahel are more vulnerable to changing climate conditions than other parts of Africa (Abdi et al. 2014; Niang et al. 2014). Increased temperature and decreased rainfall are predicted for the western Sahel in the 21st century (Roehrig et al. 2013). These potential future conditions could see the region return to the severe droughts and famines that plagued the region in the latter decades of the 20th century (Batterbury and Warren 2001; Abdi et al. 2014). Understanding the distribution and amount of GPP that enters the Sahel ecosystem is therefore important for improved understanding and quantification of the carbon cycle and climate models. And for creating more accurate early warning systems for famines in the region, as well as contribute to risk assessments for longer term deficits in resources due to declines in GPP and increases in population. Semi-arid ecosystems like the Sahel play an important role in the interannual variability of global CO_2 uptake (Ahlström et al. 2015).

One problem with estimating GPP in the Sahel is there are few sites where *in situ* data on GPP and environmental properties is available (Tagesson et al. 2015b). Satellite remote sensing is therefore an important method for collecting data on the Sahel (Tagesson et al. 2015a). The Meteosat Second Generation's Spinning Enhanced Visible and Infrared Imager (MSG/SEVIRI) and the Moderate Resolution Imaging Spectroradiometer (MODIS) are two of the satellite sensors currently used for remote sensing of GPP. The data from MODIS covers the entire Earth, while the geostationary MSG covers Africa, Europe and parts of Asia and South America.

1.1 AIM

The aim of this study is to:

1. Evaluate how well GPP can be estimated using data from the MSG/SEVIRI satellite sensor

2. Make a descriptive analysis of how GPP varies across the year in the Sahel region of Africa.

A further aim is to answer the following questions:

3. How do the satellite derived GPP compare against GPP data collected from measurement towers on the ground?
4. How does the GPP calculated from MSG/SEVIRI for the Sahel compare to the MODIS GPP product?
5. If the products provide different results, what might be the best use for each of them? (This of course depends on what questions are being asked.)

The study period was the years 2011 and 2012. These years were selected since all the necessary data was available for this time period. The field site near the town Dahra in Senegal was the only site with *in situ* GPP data for the 2011-2012 time period.

1.2 Background

The Sahel has been the subject of much environmental research since the 1970s (Batterbury and Warren 2001). For the period 1982-1990 GPP varied between years, with the inter-annual variation linked to large variations in precipitation (Myneni et al. 1995). This is expected since water is the main limiting factor in the Sahel (Running et al. 2004). For 2000-2009 GPP was stable throughout the region, based on data from MODIS and ecosystem models (Zhang et al. 2014). Olsson et al. (2005) found increasing Normalized Difference Vegetation Index (NDVI) across the Sahel for 1982-1999. This suggests an increase of green biomass for the time period. The primary driver of this greening trend was precipitation, according to ecosystem modelling done by Hickler et al. (2005). Herding, grazing and agricultural pressures did not significantly affect the vegetation dynamics in the Sahel for 1982-2002 (Seaquist et al. 2009). However, the authors note that such pressures could increase in the coming decades. More information on the Sahel can be found in section 1.3.

1.2.1 The Satellite Systems

There are a number of differences between the data from the SEVIRI and MODIS sensors. MSG/SEVIRI is in geostationary orbit over Africa and collects data every 15 minutes, which can then be integrated for longer timespans (Aminou 2002). The geostationary orbit also means that it is constantly observing the same area, so there is no time when data is not being collected.

The Terra satellite orbits the Earth in a polar orbit. Therefore the MODIS sensor has to make several orbits to completely cover the Earth. MODIS data is provided as eight day composites to reduce the effects of clouds and other atmospheric interferences. Daily data is also available. The eight day composite data was used in this study. Each data point is then only an instantaneous value from the time when the satellite passed over that point.

These differences in sensor and satellite characteristics are reflected in the data. For the same time period the size of the data files from MSG/SEVIRI are much larger than for MODIS, because the temporal resolution is much higher. MODIS has a better spatial resolution than MSG/SEVIRI. The increased temporal resolution could result in more accurate GPP estimations and results that better reflect nature. The increased amount and size of data files also requires more storage and more processing power.

1.2.2 The Carbon Cycle

The carbon cycle is the exchange of carbon between the atmosphere, biosphere, hydrosphere, pedosphere and hydrosphere of the Earth.

GPP is the total amount of carbon that is absorbed by vegetation, usually measured in g C m^{-2} d^{-1} (Chapin et al. 2002). As it is the influx of matter and energy into an ecosystem understanding GPP on large scales is important for carbon cycle studies as well as resource planning and management (Waring and Running 2007).

Environmental controls of GPP include temperature, precipitation, more directly the soil moisture, incoming radiation and nutrient availability (Traore et al. 2014). On a global scale mean annual precipitation (MAP) accounts for 72% of GPP variation (Garbulsky et al. 2010). Mean annual temperature (MAT) accounts for 45% on a global scale, mostly in northern forest ecosystems (Garbulsky et al. 2010). Nemani et al. (2003) found that precipitation was an important factor for NPP levels in dry regions and temperature is more important in high latitude colder regions.

Some of the GPP absorbed by plants is returned to the atmosphere by autotrophic respiration (R_a). R_a is the carbon that is used by plants for their metabolism. It is usually divided into growth respiration and maintenance respiration. Respiration is limited by temperature (Sitch et al. 2003) and nutrient availability (Ryan 1991) as well as water. The partitioning of R_a between growth and maintenance changes over the year, while the total R_a is stable (Falge et al. 2002)

The remaining part of the GPP is the Net Primary Production (NPP) which is the amount of carbon that a plant can use to increase its biomass and produce necessary chemicals (Chapin et al. 2002).

Carbon also leaves the ecosystem by heterotrophic respiration (R_h), which is the respiration of animals and microbes (Chapin et al. 2002). The sum of R_h and R_a is called ecosystem respiration (R_e) (Falge et al. 2002).

The balance between absorbed CO_2 and lost carbon by respiration is named Net Ecosystem Exchange (NEE) (Tagesson et al. 2015a). NEE can be directly measured with gas analysers, in contrast to GPP (Chapin et al. 2002).

1.2.3 Estimating GPP

It is not practically possible to directly measure GPP. Instead GPP has to be estimated indirectly by deriving it from e.g. remote sensing, vegetation models or *in situ* measurement of CO_2 fluxes. Satellite remote sensing has the advantage of being able to cover large areas of the Earth simultaneously and therefore giving scientists the ability to easily study large scale patterns of GPP. However, the satellite derived GPP needs to be validated against *in situ* measurements on the ground to ensure the reliability of the data.

The LUE method (Monteith 1972) is a commonly used method for estimating GPP from satellite data. The method estimates GPP by means of Photosynthetically Active Radiation (PAR), measured in MJ m^{-2} day^{-1}, the fraction of PAR that is absorbed by plants (FAPAR, unitless, 0-1), and the Light Use Efficiency (LUE, ε) in g C MJ^{-1}. Eq. 1 describes the relationship between these parameters:

$$GPP = \varepsilon \cdot PAR \cdot FAPAR \qquad \textit{Eq. 1.}$$

Where ε is the light use efficiency.

PAR is the amount of incoming solar radiation in the visible spectrum (400 – 700 nm) (McCree 1981).

PAR varies over the year as the incoming solar radiation changes. Furthermore clouds have a negative impact on the amount of PAR that reaches the ground (Frouin and Pinker 1995). Diffuse incoming radiation can also have an effect on GPP (Donohue et al. 2014). The diffuse fraction accounted for 5-10% of the accuracy of their model across coastal sites in Australia. For northern Australia, which has a monsoon season, the diffuse fraction's contribution was up to 50% (Donohue et al. 2014).

FAPAR is the fraction of incoming PAR absorbed by green plants in their canopy. FAPAR is a fundamental variable, often used in carbon and global circulation models (GCM) (GCOS 2003). In GCM's it can be used to estimate how much carbon is assimilated by plants and how much water is released due to evapotranspiration (Gobron and Verstraete 2009). It is expressed in a range from 0 – 100 %. FAPAR mainly depends on Leaf Area Index (LAI) and vegetation cover (Asrar et al. 1992). LAI is area of leaves per ground area (m^2/m^2), and vegetation cover is how much of the ground is covered by the vegetation in percent. For environments like the Sahel where the vegetation cover is often sparse, the vegetation cover is more important than LAI when determining FAPAR (Asrar et al. 1992).

LUE is the efficiency with which the vegetation converts the absorbed photosynthetic radiation into carbon. It varies widely with different vegetation types (Running et al. 2004). There is no convergence of LUE between different plant functional types (Goetz and Prince 1999). Generally, precipitation is the most important control of LUE according to Garbulsky et al. (2010), who also concludes that the annual precipitation is more important for the variation of LUE than long-term MAP. LUE increases with increasing precipitation (Garbulsky et al. 2010). Temperature can be more important than precipitation in cold regions. Nutrient availability is also a factor controlling LUE (Goetz and Prince 1999). Future increases in atmospheric CO_2 can have an effect on LUE, which is highly sensitive to CO_2 levels (Traore et al. 2014). Increased atmospheric CO_2 concentration means that less water is needed by the plants to assimilate the same amount of carbon. This increases the water use efficiency, which means that arid ecosystems can increase their uptake of CO_2 without an increase in precipitation (Poulter et al. 2014).

For *in situ* estimations the Eddy Covariance (EC) method is a standard for measuring fluxes between the atmosphere and the land on scales of ca 1×1 km, depending on sensor height, wind direction and other environmental conditions. The main problem with this method in African regions is that the number of measurement stations are limited (Sjöström et al. 2011). This is due to the expense of the equipment, lack of technical expertise and maintenance difficulties.

The EC technique measured NEE, from which GPP can be calculated using the following equation (Chapin et al. 2002):

$$GPP = NEE + R_E \qquad \textit{Eq. 2.}$$

Where R_E is the ecosystem respiration, which is the same as the NEE measured during night where there is no photosynthesis. R_e for the entire diurnal

cycle can be estimated by a temperature-based model (Chapin et al. 2002).

1.3 STUDY AREA

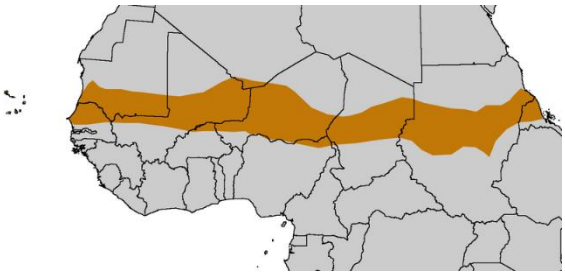

Figure 1: Location of the Sahel region in Africa. Image from Wikimedia Commons.

The Sahel is an eco-climatic region in Africa located between the Sahara desert to the north and the savannah to the south, as seen in figure 1. It stretches across the continent from Senegal in the west to Eritrea in the east. The climate is hot and dry for most of the year. The main characteristic is the rainy season between July and October (Herrmann et al. 2005). The growing season coincides with the rainy season, and the seasonal differences are strong (Herrmann et al. 2005). The annual uptake of carbon is low in comparison to other biomes (Hanan et al. 1998). During the growing season the CO_2 flux was often equal to those of other biomes (Hanan et al. 1998). The measurements of Hanan et al. (1998) peaked at 15 µmol m^{-2} s^{-1}. In comparison peak fluxes were 6-38 µmol m^{-2} s^{-1} for temperate deciduous forests, 2 µmol m^{-2} s^{-1} for a boreal forest, 16 µmol m^{-2} s^{-1} for a Brazilian tropical forest and 25 µmol m^{-2} s^{-1} in a temperate grassland (Hanan et al. 1998).

Rainfall in the Sahel is driven by the northward movement of the Inter Tropical Convergence Zone (ITCZ) (Nicholson 1981; Sultan and Janicot 2000). The ITCZ is the region where the winds from north and south of the equator converge (Chapin et al. 2002). Due to the Earth's axial tilt zone of maximum surface heating moves north and south of the equator during the year, and the ITCZ moves along with it (Lucio et al. 2012). Wetter years may be caused by the ITCZ moving further north than during regular years (Nicholson 1981).

El Niño Southern Oscillation (ENSO) affects the sea surface temperature (SST) of the Indian and Atlantic ocean (Nicholson and Kim 1997). These SST changes in turn affect the rainfall in the Sahel by changing the tropical atmospheric circulation (Folland et al. 1986). Bader and Latif (2003) found that increased SST in the Indian Ocean reduced the amount of rainfall in the west Sahel for 1950-1990. Colder SST than normal in the Atlantic or Indian Oceans increases the precipitation in the Sahel (Nicholson and Kim 1997)

There has been severe droughts throughout the last half of the 20th century (Wang and Eltahir 2000). The decreased rainfall that lead to the severe droughts of the 1970's and 1980's were not caused by movement of the ITCZ (Lucio et al. 2012). In the last decades there has been a re-greening trend in parts of the region (Dardel et al. 2014). This greening of the Sahel is caused by increased precipitation which in turn has increased the biomass, primarily in the form of a higher tree cover (Brandt et al. 2015).

While GPP showed medium to high interannual variation for 1982-1990, NPP remained unchanged for most of the Sahel during 1981-1999 (Running et al. 2004). The GPP variability stabilized in the first decade of the 21st century. During that time period NPP increased for most of the Sahel, while the global NPP decreased (Zhao and Running 2010). This is in contrast to the

findings of Zhang et al. (2014), who found a decrease of NPP in the Sahel for 2000-2009 based on MODIS data and ecosystem models, while GPP remained stable.

The soils of Africa, and especially in the Sahel, are unsuitable for agriculture (Breman et al. 2001). The sandier soils are easy to cultivate with simple tools. Heavier soils require more expensive machinery, which few farmers in the region can afford. Historically the people of the Sahel have been accustomed to using diversity and flexibility to ensure their livelihood (Batterbury and Warren 2001; Mertz et al. 2009).

1.3.1 Dahra

Image 1: View of the Dahra site February 6 2013.

The ground control data for this thesis was obtained from a measurement site located north-east of the town Dahra, Senegal (15.40 ºN, 15.43 ºW). The site is located in the Sahel region of Africa, and was established in 2002 (Tagesson et al. 2015b). The climate is hot and dry, with temperatures between 15.9 and 39.9 ºC (Tagesson et al. 2015b). Mean annual temperature is 29 ºC (Tagesson et al. 2015a). The rainy season lasts from July to October, peaking in August. For the study period the precipitation was 466 mm for 2011 and 606 mm for 2012 (Tagesson et al. 2015b). More than 95% of the annual precipitation falls during the rainy season (Tagesson et al. 2015b). The rainy season started day of year (DOY) 176 for both 2011 and 2012 and ended on DOY 278 in 2011 and 289 in 2012 (Tagesson et al. 2015b). The vegetation consists of shrubs, low trees and grasses, with a tree cover of around 3% (Tagesson et al. 2015a). The terrain is flat and extends with the same vegetation for several kilometres in all directions (Tagesson et al. 2015a).

Tagesson et al. (2015a) noted high CO_2 fluxes for Dahra compared to other semi-arid sites in Africa, with fluxes being more similar to tropical grasslands. The peak daily GPP was 15 g C m^{-2} for 2010-2013 and R_e peaked at 12 g C m^{-2} for the same period (Tagesson et al. 2015a). LUE varied between 0.02 g C MJ^{-1} in the dry season and peaked at 2.27 g C MJ^{-1} in the rainy season (Tagesson et al. 2015a). No greening or browning trend in NDVI was found for Dahra between 2002-2012 (Tagesson et al. 2015b).

2 DATA AND METHODS

2.1 DATA

The data used for the GPP calculations were from the MSG/SEVIRI sensor, which provides data in four visible and NIR channels as well as eight IR channels (Aminou 2002). The spatial resolution is 3 km at nadir, and the baseline repeat cycle is 15 min. The MSG-2 satellite upon which the SEVIRI sensor is mounted was launched in 2005 and is in an geostationary orbit (ESA 2015). The satellite data was processed by the Land Surface Analysis Satellite Applications Facility (LSA SAF) (http://landsaf.meteo.pt/) to create the Downward Surface Shortwave Flux (DSSF) and FAPAR data sets used for calculating GPP. The LSA SAF products used were

DIDSSF (daily integrated DSSF) and FAPAR.

The land cover map used to assign LUE-values was downloaded from the LSA-SAF website (https://landsaf.ipma.pt/). This land cover data was provided by LSA-SAF for use with their products. It uses the land cover definitions from the International Geosphere-Biosphere Program (IGBP) as they are defined in Belward (1996).

The data from LSA-SAF is divided into geographical regions as seen in figure 2. The data sets for North Africa (NAfr) was used since they contain the whole of the Sahel region.

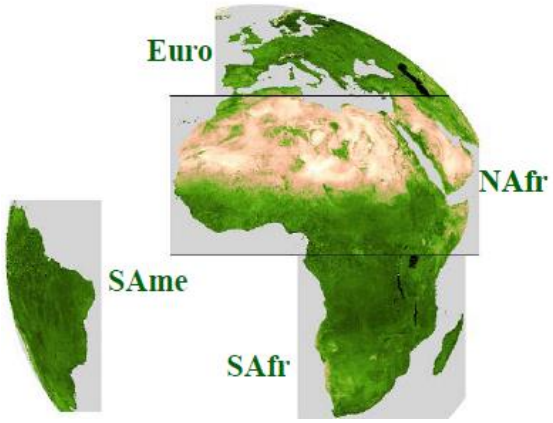

Figure 2: Geographical distribution of the LSA-SAF SEVIRI-based data sets. Image from (LSA-SAF 2011a).

The MODIS GPP data comes from the MODIS sensor mounted on NASA's Terra and Aqua satellites. It has a spatial resolution of 250, 500 or 1000 m and collects data in 36 different bands (Lillesand et al. 2008). The MOD17 GPP product used in this study has a spatial resolution of 1 km and a temporal resolution of 8 days. The evaluation data is GPP calculated from eddy covariance (EC) measurements in the Dahra field site in Senegal. The GPP was calculated from the EC data by Tagesson et al. (2015a).

Below, each data set used in the study is described. More detailed information can be obtained from the referenced documents and papers.

2.1.1 DSSF

Downward Surface Shortwave Flux (DSSF) is the radiative energy between 0.3 – 4 µm reaching the Earth in W m^{-2}. DSSF depends on the solar zenith angle, cloud cover and to a smaller degree on the surface albedo and the atmospheric absorption (LSA-SAF 2011a). The daily DSSF (DIDSSF) product used in this study is created by integrating the 30 min values for the standard product over the day.

The method used for retrieval of DSSF from the satellite data by LSA-SAF is based on the methods and developments at Météo-France (LSA-SAF 2011a). The LSA-SAF method differs from the methods from Météo-France in spatial and temporal resolutions, the source of the ancillary data and which SEVIRI channels are used (LSA-SAF 2011a). Clouds have a negative impact on the amount of DSSF reaching the surface. Therefore there are two methods with different parameterisation used for deriving DSSF data: one for cloudy skies and one for clear skies.

For clear skies the method used takes into account the scattering of radiation in the atmosphere, the spherical albedo of the atmosphere (LSA-SAF 2011a). Both the direct and diffuse, scattered by the atmosphere, incoming radiation is considered and included in the DSSF product. The equations used are from Frouin et al. (1989)

A cloud mask is used to determine if a pixel is cloudy or not. If a pixel is cloudy the DSSF estimation is done considering the effect that clouds have on radiation transfer

in the atmosphere. This is done based on methods according to Gautier et al. (1980) and Brisson et al. (1999). If a pixel is classified as cloudy it is assumed that the entire area of the pixel is covered by clouds. The cloudy skies method includes cloud transmittance in addition to atmospheric transmittance. It also includes cloud albedo and atmospheric transmittance between the cloud layer and the surface (LSA-SAF 2011a).

The DSSF and DIDSSF products have been validated by LSA-SAF prior to their release. Validation data from Mali, which is the most relevant location for this study, shows that there is an overestimation of DSSF for clear sky pixels (LSA-SAF 2011b). However, the time series for Africa have not yet been analysed in detail.

Aerosols are one source of uncertainty in the data, since it is currently included only as a simple parameter not as variable. Surface albedo on the other hand is included as a variable using the Land-SAF albedo product (LSA-SAF 2011b). Problems due to surface albedo are only expected to occur when an area is covered with snow (LSA-SAF 2011b).

For the DIDSSF product the relative errors are lower than 10 % and sometimes lower than 5 % for the North African validation sites (LSA-SAF 2011b). Underestimation of the effects of aerosols and the influence of missing data are the main sources of error in the DSSF and DIDSSF products (LSA-SAF 2011b).

2.1.2 FAPAR

LSA-SAF provides FAPAR data with daily temporal resolution, which is integrated from instantaneous FAPAR over the day. FAPAR is calculated assuming clear skies.

The algorithm used for calculating FAPAR uses directional coefficients from the Bidirectional Reflectance Distribution Function (BRDF) for the different spectral channels (Geiger et al. 2008). Negative impacts from view and sun angles to variation surface reflectance are minimized since the product is derived from the same geometry for the entire SEVIRI disk (LSA-SAF 2013).

The SAIL (Scattering by Arbitrarily Inclined Leaves) model is used to provide the BRDF data and how much radiation the vegetation absorbs (LSA-SAF 2013). Inputs for the SAIL model are leaf area index (LAI), leaf transmittance and reflectance, leaf inclination distribution and soil spectral albedo. FAPAR is derived from the calculated NDVI. (LSA-SAF 2013).

The FAPAR data has been validated by comparing it to ground data. For the Sahel region the validation was done in Dahra. Errors inherent to the model has also been considered. The product has also been compared to similar offerings from other sources (LSA-SAF 2008).

Retrieval of FAPAR is unreliable for regions such as Central Africa where persistent clouds interfere with the model (LSA-SAF 2008).

"*Another limitation of the algorithm comes from the synthetic dataset used to simulate global conditions. Although this algorithm is based on more than 5000 soil/vegetation combinations varying LAI, LIFD, soil spectral albedo and leaf optical properties for obtaining a unique global RDVI-FAPAR relationship, lambertian properties for the soil are assumed, which could introduce a systematic error for sparse canopies."* (LSA-SAF 2008).

Errors due to geometry is not a factor for the African data sets, the main source of uncertainty is instead the cloud cover (LSA-SAF 2008).

Compared to MODIS data the largest differences in FAPAR occurs in bright areas, generally corresponding to areas with bare soil or sparse vegetation (LSA-SAF 2008). Brightness due to highly reflective snow is not a problem for the African data sets (LSA-SAF 2008). The largest differences occur in deserts and semi-arid grasslands, such as in the Sahel region (LSA-SAF 2008). Validation against in situ data from Dahra for 2006 and 2007 shows that compared to MODIS the MSG/SEVIRI product might be more useful when investigating vegetation productivity and yield estimates in the Sahel (LSA-SAF 2008).

Across the Sahel region the FAPAR had optimal to medium quality in 2007. Optimal meaning a theoretical uncertainty lower than 0.1 and medium an uncertainty between 0.1 and 0.15 (LSA-SAF 2008). However in cloudy regions of west and central Africa it was lower, with uncertainties greater than 0.15 (LSA-SAF 2008). Much of the validation was done for 2006 and 2007. No new validation has been done for data collected since then.

2.1.3 MODIS GPP

The MODIS GPP (MOD17A) product is calculated from satellite-derived FPAR and estimations of PAR and LUE (Running et al. 1999). The MOD17 algorithm calculated daily GPP as:

$$GPP = \varepsilon_{max} \times SW_{rad} \times FAPAR \times f(VPD) \times f(T_{min}) \quad \textit{Eq. 3}$$

Where ε_{max} is the maximal, biome-specific light use efficiency (g C MJ^{-1}), SW_{rad} is incoming short-wave radiation (assuming 45% to be PAR), FAPAR is the fraction of absorbed PAR, f(VPD) and f(T_{min}) are linear scalars reducing GPP due to water and temperature stress.

PAR is from the MOD15 product and PAR comes from National Centre for Environmental Prediction (NCEP) along with T_{min} and VPD (Plummer 2006; Zhao and Running 2010). LUE is calculated based on parameters from biome look-up tables (BLUT) based on the land cover at launch (Running et al. 1999).

The parameters that control LUE are derived from the results of global NPP simulated with the BIOME-BGC model (Heinsch et al. 2003). LUE was then computed from this NPP together with PAR and FAPAR to generate biome specific LUE for use in the GPP calculation. (Heinsch et al. 2003).

MODIS GPP has been evaluated several times for many different biomes. It has a strong forest focus, and values for other sites might not be as representative (Plummer 2006). On a global scale GPP seasonality is captured for a large variety of climates with good results (Turner et al. 2006). In Africa the seasonality is also captured well, however GPP is underestimated for sites in the Sahel (Sjöström et al. 2013). MODIS GPP was reasonably good at replicating EC GPP across sites in Africa, but underestimated GPP consistently (Sjöström et al. 2011), especially in the Sahel. Fensholt et al. (2006) compared the MODIS NPP product with ground measurements in Senegal, and found that MODIS NPP underestimated *in situ* NPP. They found that the underestimation was due to the values in the BLUT. Underestimation of EC GPP was

also found in a coniferous forest in North America (Coops et al. 2007), however the correlation between MODIS GPP and EC GPP was strong. There is a generally poor performance during droughts and in dry areas (Plummer 2006; Turner et al. 2006; Sjöström et al. 2013).

The FAPAR value used in the model is the highest value recorded with clear skies during the 8-day period (Plummer 2006). The GPP value is therefore the maximum possible during the period, and is not representative of normal conditions (Plummer 2006).

2.1.4 *In situ* GPP data

The *in situ* GPP data was calculated from NEE, measured by EC measurements between 2010 and 2013 (Tagesson et al. 2015a). For the 2011-2012 period covered by this study there was a major loss of data between 5 November 2010 and 17 July 2011 (Tagesson et al. 2015a). Other minor breaks in the data were caused by power failures. GPP is calculated from NEE by adding R_E (Chapin et al. 2002). More details about the measurements can be found in (Tagesson et al. 2015a).

2.2 GPP Calculations

After downloading the DIDSSF and FAPAR datasets from the LSA-SAF website (https://landsaf.ipma.pt/) the first step was to extract the dates with matching datasets for FAPAR and DIDSSF. Some days did not have either of the datasets, and some had only datasets for one of DIDSSF or FAPAR. For 2011 there was 343 (94%) days with matching data, and for 2012 there was 333 (91%) days.

Since the Dahra field site was located at the border of two MSG/SEVIRI pixels the data was extracted from all the surrounding

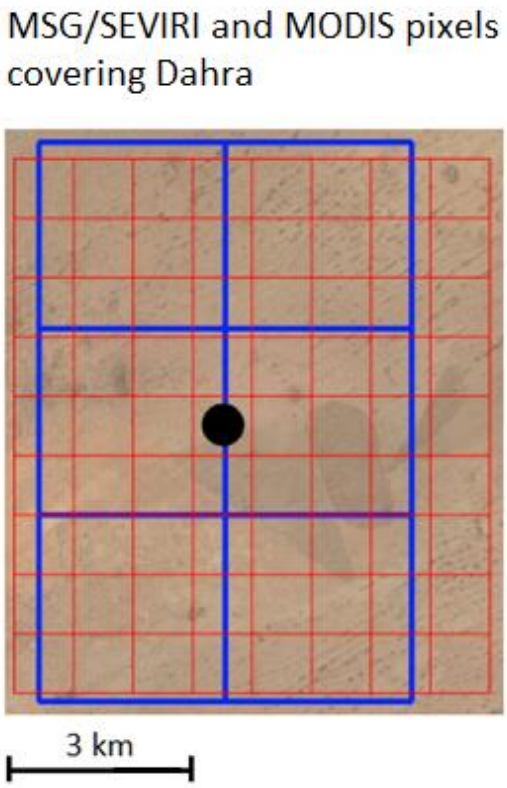

Figure 3: Approximate location of the pixels used to extract data for calculating GPP in Dahra. The blue grid represents the MSG/SEVIRI pixels, the red grid represents the MODIS pixels and the black circle is the Dahra site.

pixels, as shown in figure 3, and averaged to create a representative value for use with the evaluation against EC data. The MODIS GPP data was extracted from the area surrounding Dahra in order to cover

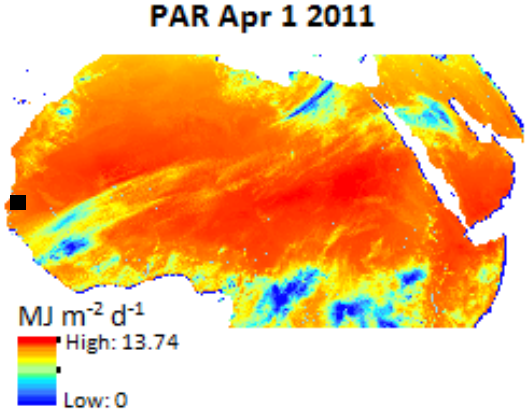

Figure 4: PAR calculated from the DIDSSF product for April 1 2011. PAR = 0.46 ×DIDSSF. The black square is Dahra.

approximately the same area as the MSG/SEVIRI pixels.

PAR was calculated to 46% of the DSSF according to Iqbal (1983). An example of daily PAR can be seen in figure 4. Note the areas of low values in blue, likely corresponding to clouds and or aerosols.

FAPAR was extracted from the downloaded files along with the theoretical errors of the product described previously. An example of daily FAPAR and its errors can be seen in figure 5 below.

LUE for the regional calculations was determined by land cover. LUE values were assigned to the different land cover classes based on the values found in Garbulsky et al. (2010). The annual average LUE for each land cover type was used. The distribution of LUE can be seen in figure 6.

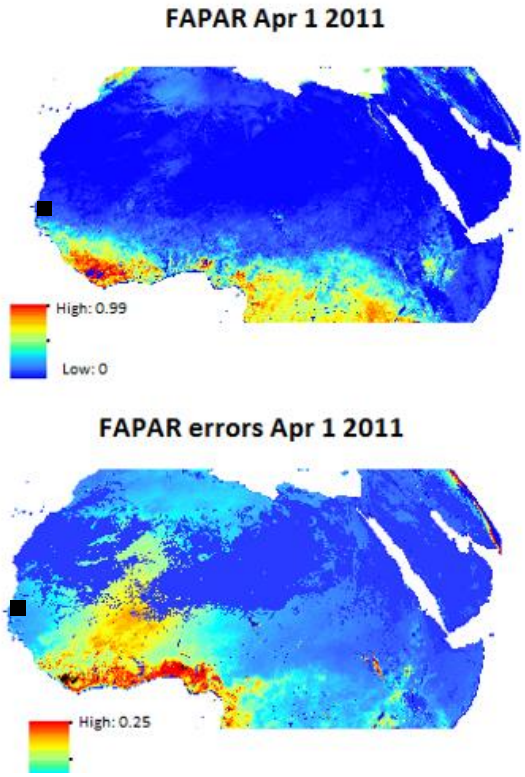

Figure 5: Shows the FAPAR and FAPAR errors from the LSA-SAF FAPAR product for April 1 2011. The value -0.06 indicates missing data. The black square is Dahra.

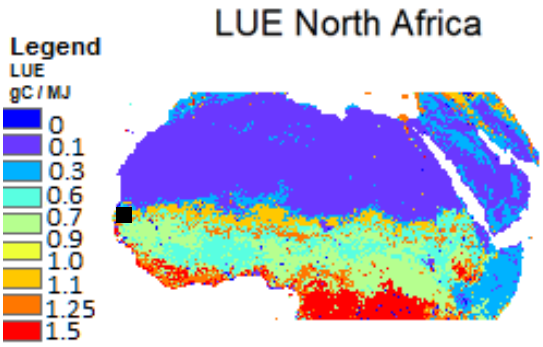

Figure 6: Shows the distribution of LUE based on land cover type. The black square is Dahra.

GPP from MSG/SEVIRI was then calculated using *Eq 1*. Regional GPP maps for a selection of dates were made for 2012 to illustrate the change of GPP before, during and after the rainy season. The final GPP for April 1 2011 can be seen in figure 7.

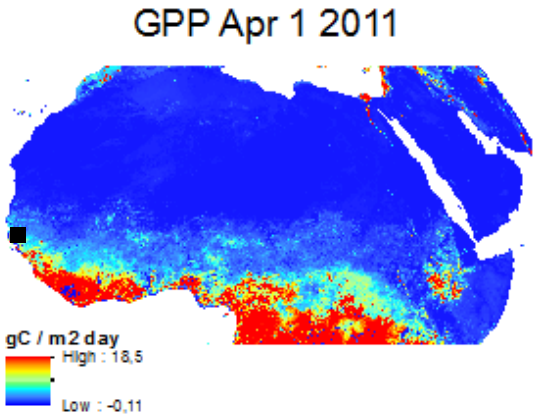

Figure 7: GPP calculated from the data shown in figures 2-4 for April 1 2011. The black square is Dahra.

For the Dahra site GPP was calculated from the extracted PAR and FAPAR values with a LUE value of 1.2 g C MJ^{-1}, an intermediate value between the highest and lowest values for savannahs and grasslands according to (Garbulsky et al. 2010) and also between the highest and lowest noted for Dahra by Tagesson et al. (2015a), as mentioned earlier.

The FAPAR error product was used to calculate the highest and lowest possible GPP values due to possible errors in FAPAR. After calculating the GPP for the Dahra site the results for days that had been

flagged as erroneous, from the DSSF product were removed. In total 2 such dates were removed.

2.2.1 Statistics

The mean absolute error (MAE), mean bias, root mean square error (RMSE) and correlation coefficient (*r*) were calculated for MSG/SEVIRI derived GPP and MODIS GPP compared to the *in situ* EC-derived GPP. In addition the annual mean value and variance for the three data sets were calculated.

In the following equations *x* is the satellite derived GPP, *y* is the EC GPP, *n* is the sample size, s_x is the standard deviation of the satellite GPP and s_y is the standard deviation of the EC GPP.

$$MAE = \frac{1}{n}\sum_{i=1}^{n}|x_i - y_i| \qquad Eq.\ 4$$

MAE, formula in Eq. 4, is a measure of how close the satellite derived GPP values are to the EC GPP values. It does not give any information on whether the satellite GPP values are higher or lower than EC GPP. The closer the satellite GPP is to the EC GPP, the lower the MAE.

$$Bias = \frac{\sum_{i=1}^{n}(x_i - y_i)}{n} \qquad Eq.\ 5$$

Bias, formula in Eq. 5, is a measure to see if there are any systematic errors between the satellite GPP and EC GPP. A bias of 0 would mean that there is no systematic error, a positive bias would mean that the satellite GPP tends to overestimate the EC GPP while a negative bias would indicate that the satellite GPP underestimates the EC GPP.

$$RMSE = \sqrt{\frac{\sum_{i=1}^{n}(x_i - y_i)^2}{n}} \qquad Eq.\ 6$$

RMSE, formula in Eq. 6 is a measure of how accurate the satellite GPP is compared to the EC GPP. The lower the RMSE the less difference there is between the satellite GPP and the EC GPP.

$$r = \frac{\sum_{i=1}^{n}(x_i - \bar{x})(y_i - \bar{y})}{(n-1)s_x s_y} \qquad Eq.\ 7$$

The correlation coefficient, Eq. 7, measures of how strong of a linear relationship there is between two variables. It ranges from -1 to +1, where -1 is a perfect negative linear relationship and +1 is a perfect positive linear relationship. A value of 0 means that there is no linear relationship between the two variables. A value of *r* close to +1 is desired in this study. However, even though the correlation is good it does not mean that the satellite GPP is accurate compared to the EC GPP. The *r*-value is influenced by the size of the sample. The larger the sample, the lower the absolute *r*-value needs to be for significance (Rogerson 2010). For this study the MODIS GPP with a sample size of $n = 46$ needs an *r*-value of >0.361 for significance, while MSG/SEVIRI GPP with $n > 300$ needs an *r*-value of >0.124 (Rogerson 2010)

Accurate satellite estimation of GPP would therefore have a low MAE, bias and RMSE with an *r*-value close to +1. The mean value and variance should also be close to those of the EC GPP.

3 Results

3.1 2011

Figure 8 shows the result of the GPP calculations for the Dahra site for 2011. A larger version of figure 8 can be found in appendix A1. For this year there was no EC data for the first months of the year, meaning that all comparisons between *in situ* GPP and satellite derived GPP are done only for the growing season and the beginning of the dry season.

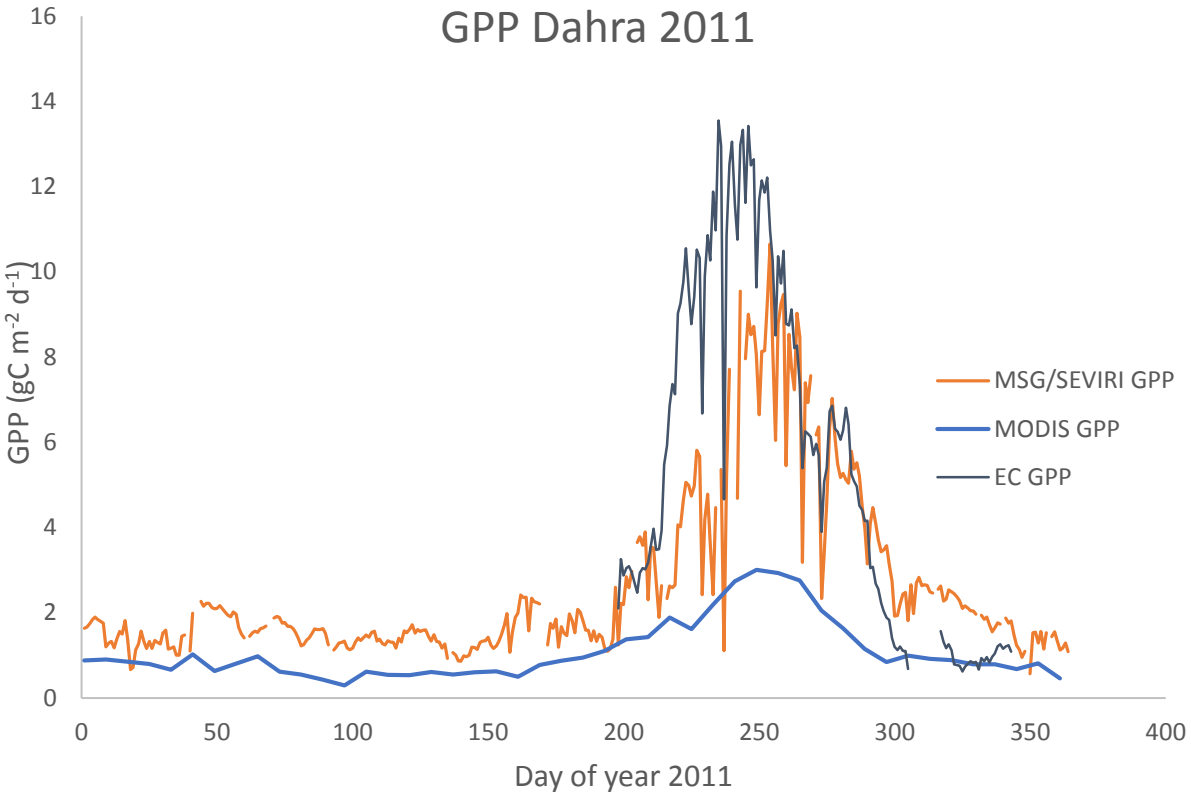

Figure 8: GPP of 2011 for the Dahra field site from MSG/SEVIRI, MODIS and in situ *measurements. Gaps in the graphs indicate periods of missing data.*

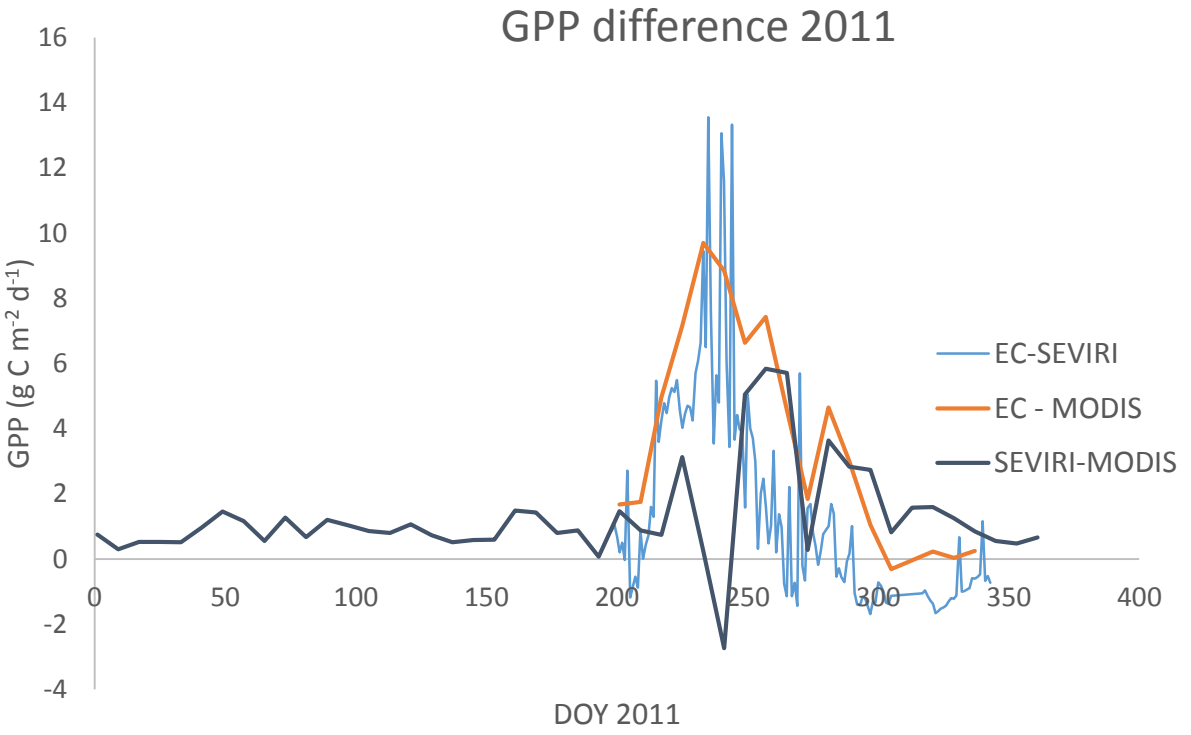

Figure 9: Difference in GPP values between MSG/SEVIRI derived GPP, MODIS GPP and EC GPP for the Dahra field site in 2011.

MSG/SEVIRI GPP show much day-to-day variance, as does the EC GPP. Though, as seen in figures 8 and 9 the variations does not always match in timing of magnitude. If they did the EC-SEVIRI graph in figure 9 would be 0 or close to 0 throughout 2011.

MSG/SEVIRI lags behind the *in situ* measurements during the early growing season, and it fails to capture the peak values. Towards the end of the growing season the MSG/SEVIRI GPP seems to match the EC GPP better, as the EC-SEVIRI graph in figure 9 is closer to 0. Figure 9 also shows a large difference between MSG/SEVIRI GPP and EC GPP between DOY 235 and 244. Apart from this peak the difference between EC GPP and MSG/SEVIRI GPP is lower than the difference between EC GPP and MODIS GPP.

Since MODIS has values every eight days it cannot match the day-to-day variance of the EC GPP. As seen in figure 8, MODIS GPP fails to reach the same maxima as the *in situ* data does. It stays consistently lower than MSG/SEVIRI GPP during the dry season. For the time between about DOY 300-350 the MODIS GPP matches the EC GPP more closely than the MSG/SEVIRI GPP. Despite not being able to capture the same values as the *in situ* measurement the start and end of the growing season is captured well (figure 8).

Figure 9 shows that MODIS GPP underestimates EC GPP for the entire growing season, and apart from the peak around DOY 240, underestimates EC GPP more than MSG/SEVIRI GPP does. However, it performs better than MSG/SEVIRI for the start of the dry season where the EC-MODIS graph is almost 0 while the EC-SEVIRI graph overestimates EC GPP (figures 8 and 9).

Maximum GPP occurs in DOY 235 for the EC GPP with a value of 13.55 g C m^{-2} d^{-1}. For MS/SEVIRI GPP it occurs in DOY 254 with a value of 10.66 g C m^{-2} d^{-1}. For MODIS GPP it occurs in DOY 249 with a value of 3.01 g C m^{-2} d^{-1}.

Figure 10 shows the MSG/SEVIRI derived GPP and MODIS GPP compared with the EC GPP. For low values the MSG/SEVIRI overestimates the *in situ* GPP, while for the higher values it underestimates them, showing that it has a lower dynamic range

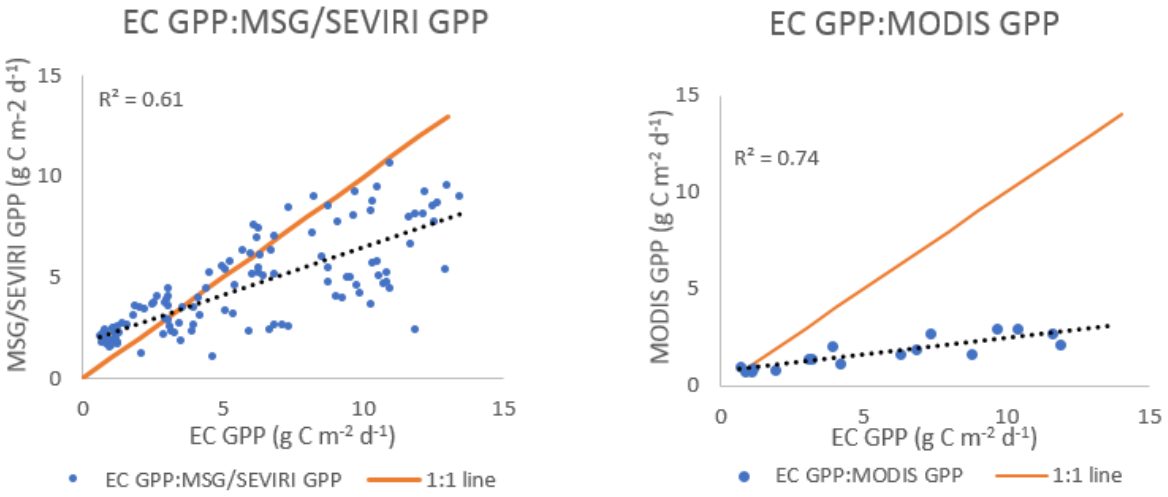

Figure 10: EC GPP plotted against MSG/SEVIRI GPP and MODIS GPP. The dotted line is the regression line between the EC GPP and the satellite derived GPP values. n=343 for MSG/SEVIRI GPP and n=46 for MODIS GPP

than EC GPP. Note that for 2011 there was EC data only for the growing season so this figure does not show MSGSEVIRI/GPP over the entire year. MODIS GPP has a higher R^2 value than MSG/SEVIRI GPP. However, the underestimation seen in figures 8 and 9 is clearly visible here. According to figure 10 MODIS GPP is only accurate for the lowest GPP values.

3.2 2012

The GPP for 2012 from the three sources for Dahra can be seen in figure 11. A larger version is available in the appendix. For this year there was EC data for most of the dates, meaning that a comparison between the two satellite products and the *in situ* data can be made for the dry season as well. Similarly to 2011 the results for 2012 the MODIS GPP products does not reach the high GPP values of the growing season (figure 11).

MSG/SEVIRI GPP is more accurate at estimating the high values of the growing season as seen in figure 11. There appears to be three distinct peaks of GPP during the growing season. The first one at ca DOY 215, the second one at ca DOY 230-250 and the last one at ca DOY 280. There is a distinct drop in GPP between the second and third peak, which is visible for both MSG/SEVIRI GPP and the MODIS GPP.

The MSG/SEVIRI GPP seem to replicate the EC GPP more accurately when it comes to the growing season, including the observed peaks. As with 2011 the MSG/SEVIRI GPP lags behind during the start and end of the growing season, which MODIS GPP seem to capture more

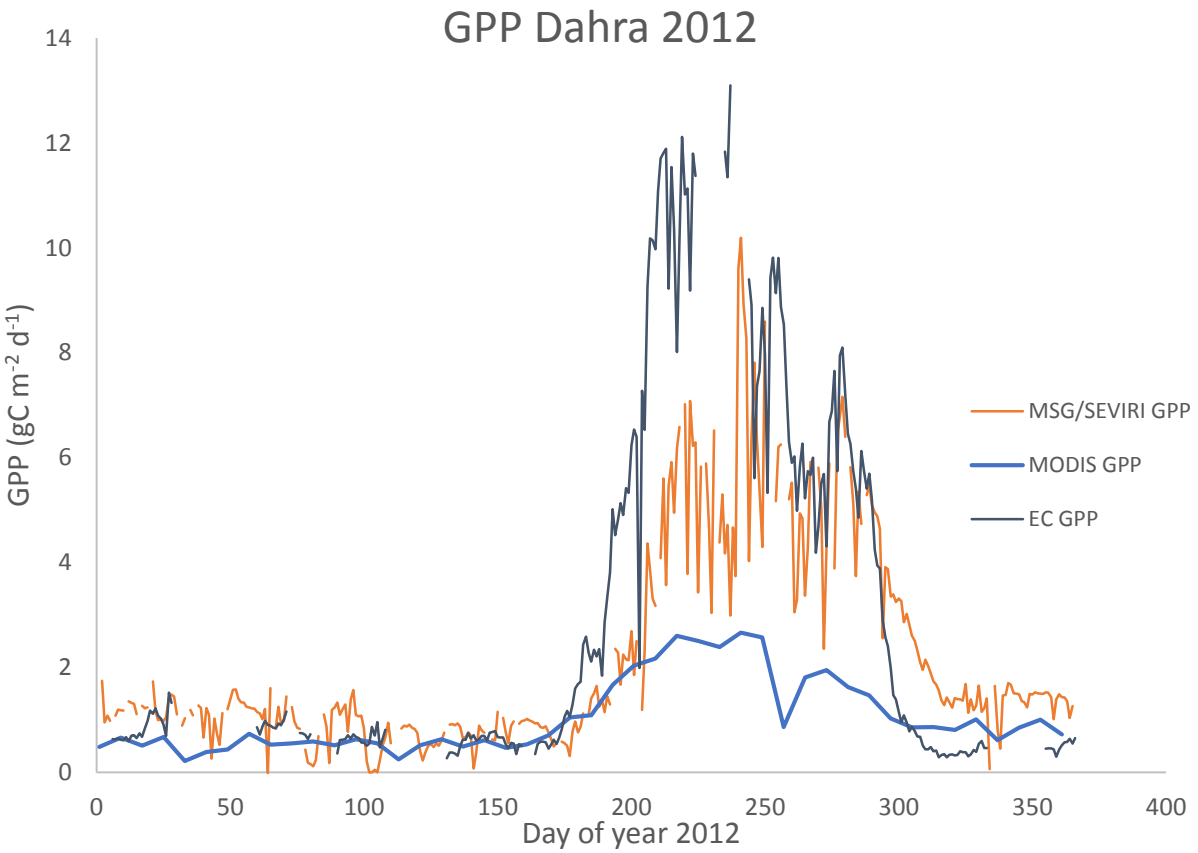

Figure 11: GPP of 2012 for the Dahra field site from MSG/SEVIRI, MODIS and in situ measurements. Gaps in the graphs indicate periods of missing data.

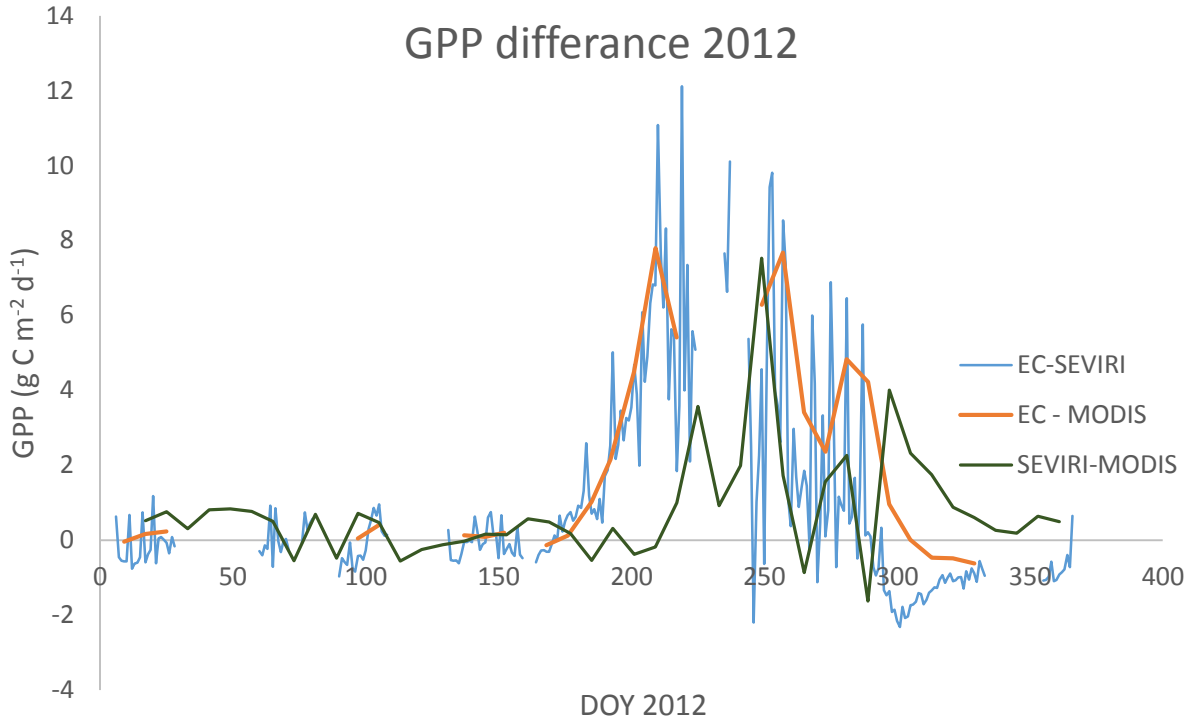

Figure 12: Difference in GPP values between MSG/SEVIRI derived GPP, MODIS GPP and EC GPP for the Dahra field site in 2012. Gaps in the graphs indicate periods where missing data made comparisons impossible.

accurately. As seen in figures 11 and 12 MSG/SEVIRI GPP underestimates GPP for the first half of the growing season, and is more similar to MODIS GPP than the EC GPP. In figure 12 the EC-SEVIRI and EC-MODIS graphs show an increasing underestimation for the first half of the growing season, while the SEVIRI-MODIS graph stays around 0.

For the latter half of the growing season MSG/SEVIRI GPP is more similar to EC GPP than MODIS GPP is (figure 12), however there are several days when the difference spikes to reach high values, meaning it underestimates EC GPP. When the dry season starts MODIS is more accurate than MSG/SEVIRI, as seen in figure 12 where MSG/SEVIRI reaches values further from 0 than MODIS GPP does. For the dry season there are large gaps and it is difficult to see any clear results. However, looking at both figures 11 and 12 MODIS GPP seems to perform slightly better than MSG/SEVIRI GPP during the dry season.

Figure 13 above shows the MSG/SEVIRI GPP and MODIS GPP compared to the EC GPP for 2012. MSG/SEVIRI GPP shows the same low dynamic range compared to EC GPP as seen for 2011.

Figure 13 also show the large deviation of MODIS GPP compared to EC GPP that can be seen in figure 11. For the lower values of the dry season it is accurate, and does not overestimate them as MSG/SEVIRI GPP does.

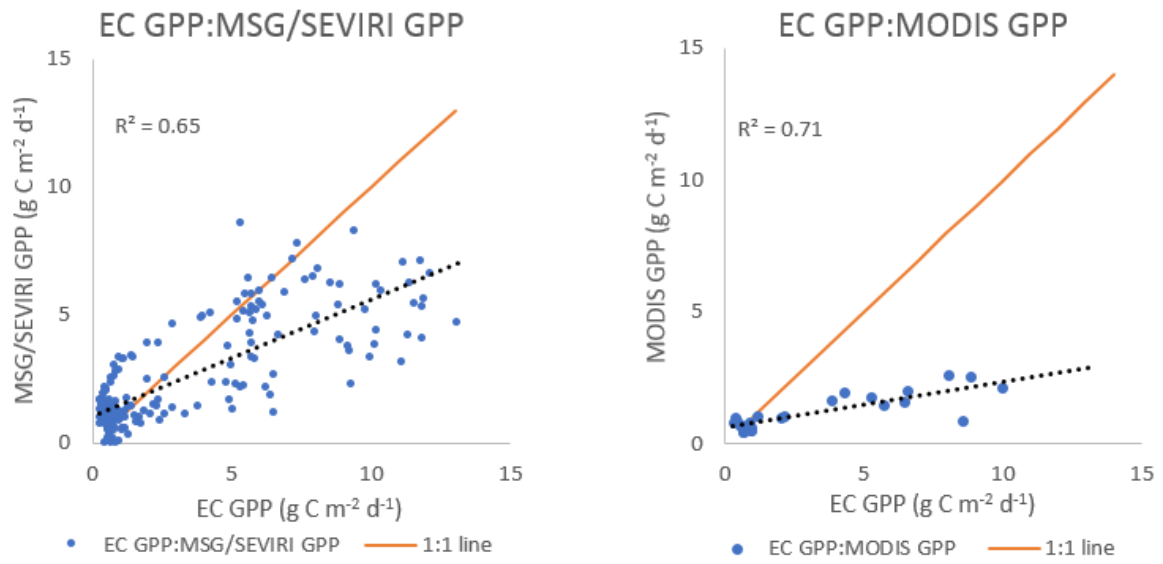

Figure 13: EC GPP plotted against MSG/SEVIRI GPP and MODIS GPP. The dotted line is the regression line between the EC GPP and the satellite derived GPP values. n=333 for MSG/SEVIRI GPP and n=46 for MODIS GPP

The daily GPP for a selection of dates from the latter half of 2012 are shown in figures 14 and 15. The images below each map were taken with a digital camera from measuring tower at the Dahra site, showing how the landscape changes throughout the growing season.

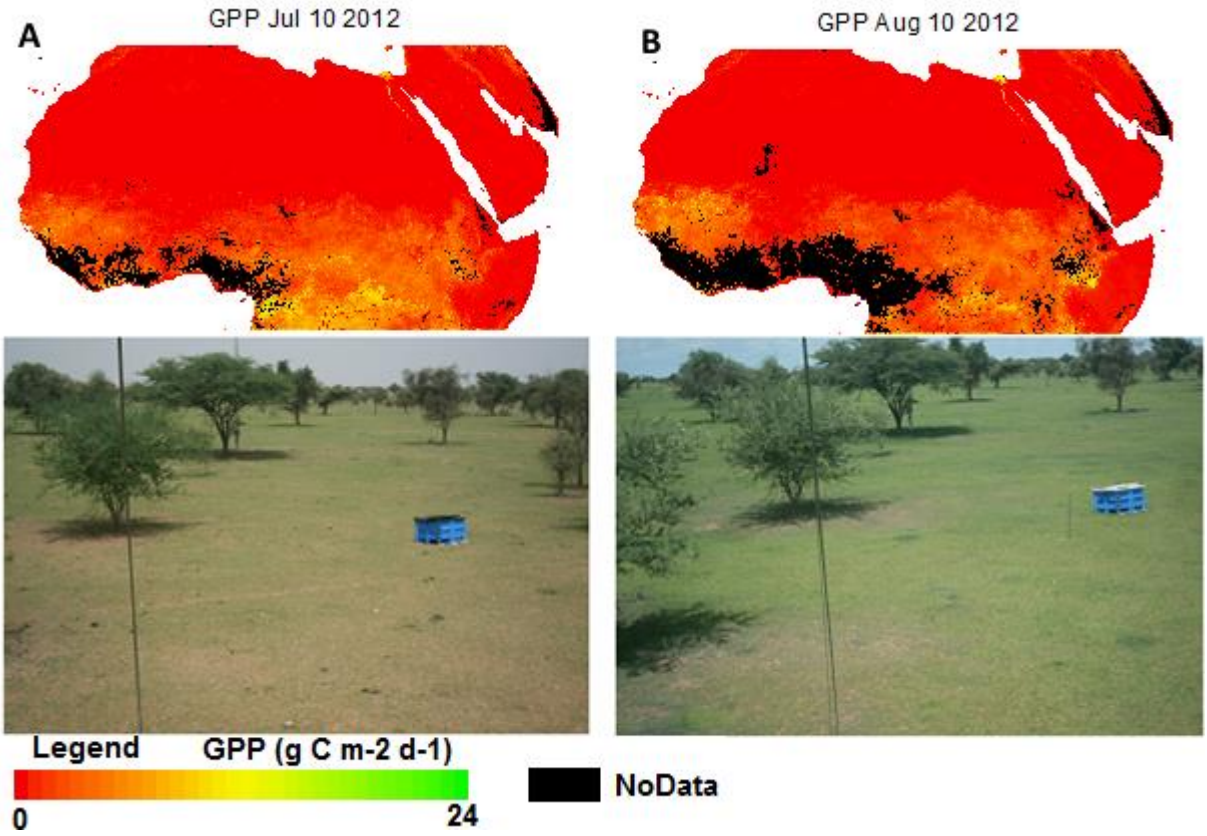

Figure 14: GPP distribution across northern Africa in 2012along with images taken at the Dahra field site for the same date, July 10 for subfigure A and August 10 for subfigure B.

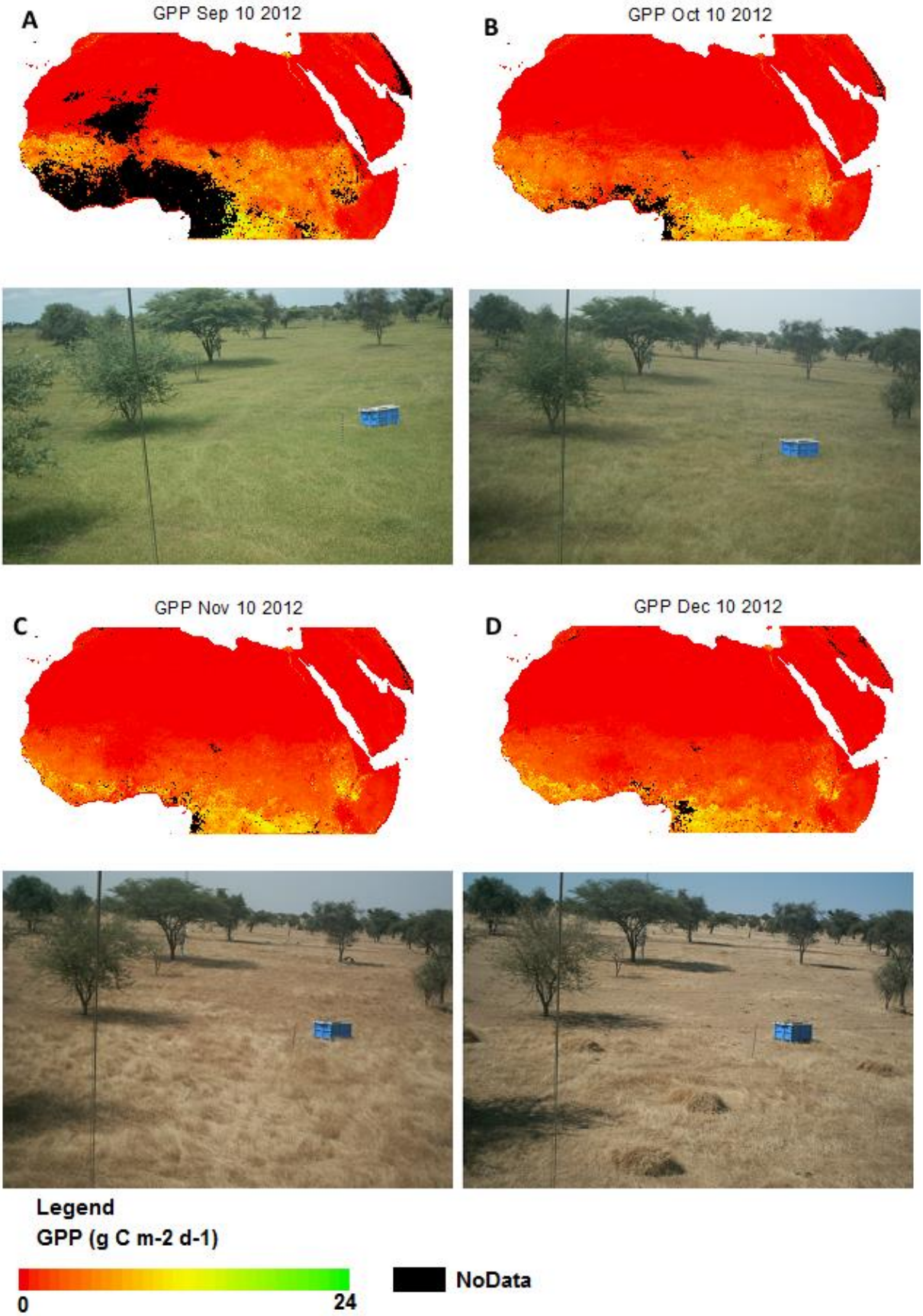

Figure 15: GPP distribution across northern Africa in 2012 along with images taken at the Dahra field site for the same date, September 10 for subfigure A, October 10 for subfigure B, November 10 for subfigure C and December 10 for subfigure D.

July 10 (DOY 192) is 16 days after the start of the rainy season in DOY 176, and the greening of the landscape can be seen (figure 13). After the end of the rainy season in DOY 289 (October 15) the rapid decrease of GPP as seen in figure 11, can be seen in figure 15 where November and December are markedly less green than the previous months seen in figure 14.

The regions of along the southern coast of West Africa and near the equator in Central Africa are marked in black due to NoData flag in the FAPAR data set. This lack of data is especially clear in figure 14(B) and 15(A), and is present in for all subfigures. NoData regions are also present across the Sahara desert in many figure 15(A). The presence of errors in the Sahara is less likely to impact the results since there is almost no photosynthetic activity there.

3.3 Entire period (2011-2012)

Figure 16 below shows the GPP from the three sources for the entire period January 1 2011 to December 2012. When viewed together there are some differences, and similarities, in the patterns of GPP between the two years which become more apparent.

The delay in the start of the growing season for MSG/SEVIRI GPP is apparent. Also the difference between MODIS GPP and MSG/SEVIR GPP during the dry season, where MODIS GPP seems to be more accurate at the actual values, while the MSG/SEVIR GPP is more accurately matching the day-to-day variation.

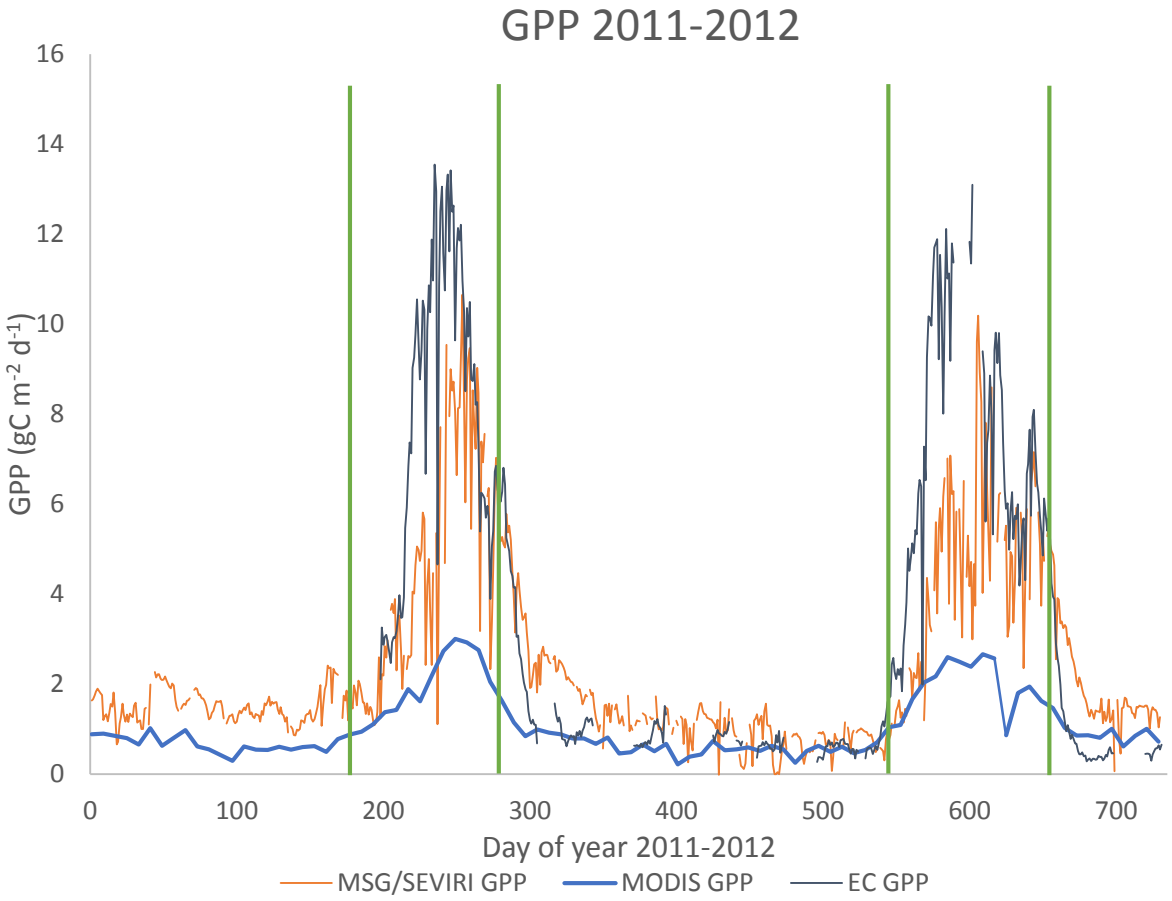

Figure 16: MSG/SEVIRI GPP, MODIS GPP and EC GPP for 2011 ad 2012 for the Dahra field site. Gaps in the graphs indicate periods of missing data. The vertical lines represent the start and end of the rainy season for the two years.

Table 1: Means, variances (Var), bias, mean absolute errors, root mean square errors and correlation coefficients for MSG/SEVIRI GPP, MODIS GPP and EC GPP. Correlations are between satellite data and in situ *data. Apart from* r *the units are in g C* m^{-2} d^{-1}.

MSG/SEVIRI	Mean	Var	Bias	MAE	RMSE	*r*
2011	2.59	4.05	-1.21	1.99	2.98	0.78
2012	2.14	3.86	-0.62	1.37	2.11	0.80
MODIS						
2011	1.08	0.47	-3.41	3.45	4.55	0.86
2012	1.04	0.49	-0.96	1.61	2.72	0.84
EC GPP						
2011	5.65	16.25	---	---	---	---
2012	3.05	12.03	---	---	---	---

Table 1 shows the computed bias, errors, correlation coefficients as well as annual mean and variance for the three data sets used in this study. It should be remembered that for 2011 most of the available EC GPP was for the rainy season, so the values for 2011 in table 1 are mostly a comparison of how the two products perform during the rainy season. For 2012 there was *in situ* data for the entire year, and the values for 2012 are therefore more accurate when evaluating performance throughout the year compared to 2011.

The MSG/SEVIRI GPP has a higher mean and variance compared to MODIS GPP, and both are lower than the EC GPP (table 1). Especially the variance is much higher for the EC GPP. 2012 shows lower values compared to 2012 for all three data sets.

The MAE and RMSE are lower for MSG/SEVIRI GPP than for MODIS GPP, with lower values for 2011 compared to 2012. There is also less difference between the two products for 2012 compared to 2011.

MODIS GPP's underestimation of EC GPP during the growing season can be seen in table 1, especially for 2011 where the bias of MODIS shows a strong tendency for lower values for MODIS GPP compared to EC GPP. Both MSG/SEVIRI GPP and MODIS GPP have negative bias for both 2011 and 2012.

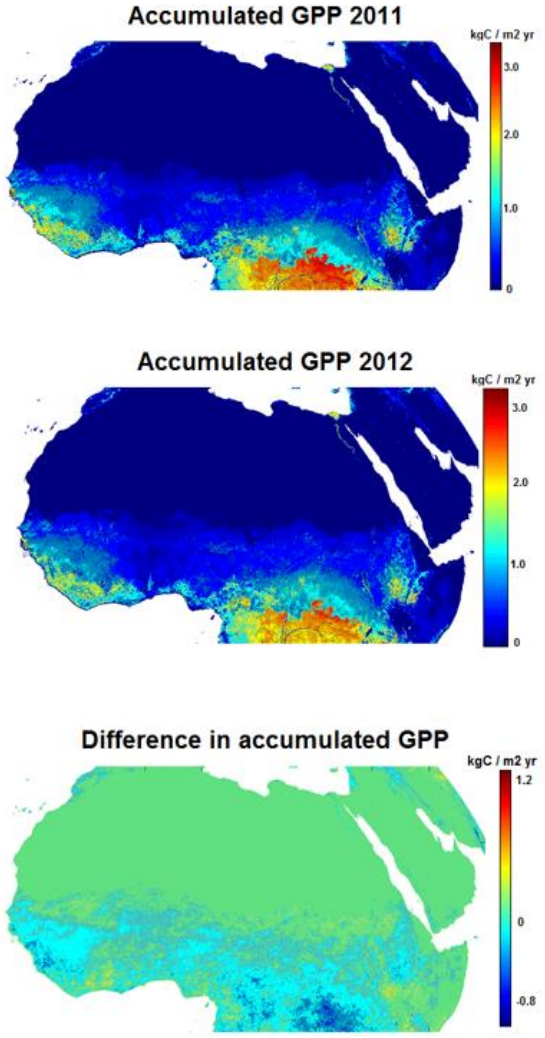

Figure 17: Accumulated GPP for 2011 and 2012 calculated from MSG/SEVIRI data. The difference between the two years is also shown (ΔGPP = GPP2012 - GPP2011).

Figure 17 shows the accumulated GPP calculated with the data from MSG/SEVIRI. The distribution of GPP is similar between the two years, with a general north-to-south gradient of increasing GPP. The highs and lows are similar between the years. As can be seen in the bottom map of figure 17 the values for the southern half of the region, especially in the rainforests near the equator, are lower for 2012 than 2011. Across the Sahel there are patches of lower and higher values for 2012 compared to 2011.

Table 2: Accumulated GPP from the MSG/SEVIRI, MODIS and in situ *datasets. Note that EC GPP for 2011 only contains data from the latter half of the year. Units are in kg C m^{-2} yr^{-1}.*

Year	MSG/SEVIRI GPP	MODIS GPP	EC GPP
2011	0.89	0.40	0.76
2012	0.70	0.38	0.78

These findings are reflected at the site in Dahra. The values for MSG/SEVIRI GPP are lower for 2012 than for 2011, as seen in table 2. The accumulated MODIS GPP for Dahra is far lower than either the MSG/SEVIRI derived GPP or the *in situ* measurements, which is consistent with the other findings of the study.

4 DISCUSSION

4.1 MSG/SEVIRI GPP

As seen in table 1 the MSG/SEVIRI GPP outperforms the MODIS GPP in all the calculated statistics apart from the correlation coefficient. The differences are smaller for 2012 than for 2011 (table 1). The lower correlation coefficient for MSG/SEVIRI GPP is likely due to the larger number of data points (n = 343 for 2011 and n = 333 for 2012 for MSG/SEVIRI data, compared to n = 46 for MODIS data). According to the guidelines in Rogerson (2010) both *r*-values are above the significance level, based on the number of observations, of 0.361 for MODIS GPP and 0.124 for MSG/SEVIRI GPP. The larger variance within the data likely explains the lower *r*-value. This can be seen in figures 10 and 13.

Figures 8-13 also show that the calculated MSG/SEVIRI GPP tends to overestimate the *in situ* GPP during the dry season, where GPP is low, and underestimate the higher values during the rainy season. One reason for this could be the use of a static LUE throughout the year. LUE has been shown to vary over the year, with higher values during the rainy season in a Sahel environment (Ardö et al. 2008; Traore et al. 2014).

A more accurate model for LUE would incorporate the effects of temperature and precipitation, which limit of LUE. This type of model is used in MOD17 and several other GPP models. One such model is used by Gilabert et al. (2015) and uses actual and potential evapotranspiration to limit LUE due to water stress. Such a model could not be used in this study due to lack of data for 2011 and 2012. An intermediate value of 1.2 g C MJ^{-1} for LUE was used instead, which could account for some of the observed over- and underestimation of GPP. Specifically LUE should be lower than 1.2 g C MJ^{-1} during the dry season and higher, reaching a peak 2.27 g C MJ^{-1} in the rainy season (Tagesson et al. 2015a).

The FAPAR product used can also account for some of the observed difference due to limitations in the model for areas with open canopies, such as the Sahel and savannah environments (LSA-SAF 2008). The assumed Lambertian soil properties which can be a source of systematic errors in sparse canopy environments can also have an effect on the calculated GPP (LSA-SAF 2008). The MSG/SEVIRI FAPAR product has also been shown to have more intermediate values in contrast to the better representation of the range of high and low values in the MODIS FAPAR product, in the Iberian peninsula (Martínez et al. 2013).

The DSSF product used in the study has been shown to overestimate values during clear skies (LSA-SAF 2011b), which could be one of the reasons behind the overestimation of lower GPP values, since low values mostly occur during the dry season when there is less cloud cover.

As seen in figure 14(B) and 15(A) there are large areas of missing data in coastal regions near the Gulf of Guinea and the equator. Since the missing data is present in large scale only during the rainy season the reason for them is likely clouds. This problem of missing data on large areas during cloudy conditions has likely also affected the result of the accumulated GPP shown in figure 17. The Sahel region, which is this study's main concern, is less affected by large-scale missing data than more southern regions. Likewise, the large areas of missing data in the Sahara does not affect the MSG/SEVIRI sensor's performance in the Sahel, but could be important for studies of Africa covering the affected areas.

The large error interval seen in 2012 (figure A2 in the appendix) between ca DOY 60 and DOY 220 are caused by unknown factors. There are no quality flags present for that time period. The three peaks of GPP in 2012 seen in figure 11 could correspond to periods of increased rainfall, or the opposite, periods during the rainy season with lower than normal precipitation. Based on fig. 2 in Tagesson et al. (2015b) the second alternative seems more likely.

There have not been many previous studies using MSG/SEVIRI data to calculate GPP. One study by Martínez et al. (2015) compared MSG/SEVIRI derived GPP with MODIS GPP, and EC GPP for two African sites: Demokeya in Sudan and Mongu in Zambia. The results of the study are similar to this one. In the Sahel site of Demokeya MSG/SEVIRI better reproduced variation and magnitude of GPP while, MODIS shows the same underestimation during the growing season (Martínez et al. 2015).

4.2 MODIS GPP

According to figures 11 and 12 the MODIS GPP product seems to perform well during the dry season in 2012. However, since GPP is so low during this period that it sometimes is ignored this is not of great importance. The low levels of photosynthesis during this period mostly come from trees with deep roots, able to reach groundwater aquifers or plants that are able to store water.

For 2011 there was no EC GPP data for much of the dry season, so interannual comparison is not possible. Figures 10 and 13 show that MODIS GPP is more accurate for lower GPP than higher for both years though. The lack of variation over time as seen in figures 8 and 11 as well as the low variance seen in table 1 is likely a result of the lower temporal resolution of MODIS compared to the EC GPP or the MSG/SEVIRI derived GPP.

The main issue with MODIS GPP in the Sahel is the severe underestimation of GPP during the growing season compared to the *in situ* GPP and the MSG/SEVIRI GPP. In 2012 it only reaches around 25-30 % of the EC GPP during the growing season. Table 1 shows that MODIS GPP performs poorer than MSG/SEVIRI derived GPP for all the calculated statistics apart from the correlation coefficient. The reason for the higher *r*-value is likely that the variance within the data set is lower, and that it has fewer data points compared to MSG/SEVIRI. The accumulated GPP shown in table 2 is also lower than for the other two data sets.

This underestimation of GPP in the Sahel by MODIS has been observed by Sjöström et al. (2011) who found that MODIS GPP underestimated EC GPP with 36% in the Sahel and southern Africa. At the most the underestimation was 64% which is a similar figure to in this study. Sjöström et al. (2013) also found that for 2000-2009 MODIS GPP underestimated EC GPP, especially in dry areas. However, seasonality is captured well. Sjöström et al. (2013) suggests that

improved driver data, FAPAR and higher maximum LUE could improve the performance of MODIS GPP in Africa.

A study by Kanniah et al. (2009) in a savannah in northern Australia found that the MODIS GPP algorithm performs poorly in water limited conditions, such as the Sahel. The main cause for differences between EC GPP and MODIS GPP in this study was found to be the FAPAR product used in the MODIS algorithm. Including soil moisture in the LUE model improved the results (Kanniah et al. 2009). Poor performance of the MODIS GPP product in water limited sites has also been observed by (Leuning et al. 2005; Heinsch et al. 2006).

The poor performance of MODIS in the Sahel is not as pronounced in other biomes, but still present at high GPP values when compared with EC GPP data (Zhang et al. 2012). Good correlation, but underestimation of 30% compared to EC GPP was found by Coops et al. (2007) studying Douglas firs in Canada. Turner et al. (2006) found that MODIS GPP responds well to trends and levels of GPP, but tended to underestimate high productivity, and overestimate low productivity.

4.3 Improvements and Issues

LUE in this study was parameterized based on land cover for the regional GPP calculations. The results could likely be improved by using more accurate LUE values. Studies focusing on LUE use remote sensing data of FAPAR combined with EC GPP and/or GPP from ecosystem models in order to calculate LUE, such as in Traore et al. (2014) and Moreno et al. (2012). Using this method to derive LUE for use in GPP calculations such as in this study would involve dividing the *in situ* GPP data between evaluating the GPP calculations and for deriving LUE for use in the model. This would be a problem for GPP calculations in the Sahel due to the low amount of *in situ* measurement stations (Sjöström et al. 2011).

Another method for using satellite remote sensing to estimate LUE was used by Drolet et al. (2008). That study used the MODIS Photochemical Reflectance Index (PRI) and MODIS FAPAR products for calculating LUE in a Canadian boreal forest. However, they concluded that new sensors designed for remote sensing of LUE was required for achieving good results (Drolet et al. 2008). New sensors designed for LUE would be useful for studies in Africa where *in situ* measurements of LUE are sparse.

One problem with the study is the lack of *in situ* measurement stations that are used to ensure that the satellite derived GPP is accurate. There are more sites in the Sahel than Dahra, as seen in Sjöström et al. (2013). Data from these sites was not available for use during the 2011-2012 time period for different reasons. For other time periods and in the future more *in situ* data might be available.

The LSA-SAF FAPAR and DIDSSF products have some issues that could have had an effect on the results. Some of these has been discussed earlier. The FAPAR product has not been validated since 2007, the data was deemed to be of medium to optimal quality for the Sahel (LSA-SAF 2008). However, newer validation could help ensure the quality of the product. The validation report for the DIDSSF product is from 2011, the same year as the start of the study. Therefore the quality assessment should be more accurate for the study period.

An assumption that has been made throughout this study is the EC GPP represents ground truth. However, the EC GPP measurements are not free of error.

Different wind conditions during the diurnal cycle can affect the results, and cause random and or systematic errors (Heinsch et al. 2006). According to Sjöström et al. (2011) tower GPP values are an adequate method of estimating local conditions if the landscape around the tower is homogenous, as it is in the vicinity of Dahra.

4.4 SUMMARY

The aim of this study was to evaluate how well GPP can be estimated using data from the MSG/SEVIRI satellite sensor for the Sahel region of Africa. In addition the resulting GPP would be compared against the commonly used MODIS GPP product MOD17A in order to evaluate which one performed best. The GPP from both sources was compared against *in situ* GPP estimations using eddy covariance data from the Dahra field site in Senegal.

The result show that GPP calculated from the MSG/SEVIRI data performed better than MODIS GPP in capturing the day-to-day variations seen in the EC GPP. It was also more accurate in estimating the high values reached during the growing season, though it underestimated the EC GPP values. On the other hand MSG/SEVIRI GPP had some issues during the dry season when GPP was overestimated for the lowest values. However, since GPP is almost 0 for the dry season this is not a major issue.

MODIS GPP performed well during the dry season and in capturing the change between dry and rainy season GPP. However, it failed to reproduce the high values of the growing season, generally underestimating them by 25-30%. Total accumulated GPP for the Dahra field site was lower than the EC GPP and the MSG/SEVIRI GPP.

GPP across the Sahel was calculated from MSG/SEVIRI data. However, it was not possible to evaluate its performance across the region due to the lack of sites with *in situ* data available for the study period. There were problems with clouds for regions further south (figures 14 and 15) but the impact on the Sahel from the clouds was likely minor. Dahra has been noted to have high productivity, and therefore the underestimation of GPP at Dahra might not be reflected at other sites. This will require further studies with other sites to confirm.

As part of the aim of this study, three questions were asked concerning the performance of MSG/SEVIRI derived GPP and MODIS GPP; and how they compared to *in situ* GPP estimated using the eddy covariance method.

1. *How does the satellite derived GPP compare against GPP data collected from measurement towers on the ground?*

Compared to the *in situ* EC GPP the MSG/SEVIRI derived GPP was better at replicating the results from the Dahra site. The accumulated GPP was more similar to the EC measurements, the day-to-day variation was captured more accurately and the actual daily GPP levels were more similar. However, MSG/SEVIRI GPP tend to overestimate GPP during the dry season and underestimate it during the rainy season.

MODIS GPP proved to be well suited for capturing seasonal changes, perhaps more so than MSG/SEVIRI GPP regarding the start and end of the growing season. However, the GPP values from the MODIS GPP product was lower than the EC GPP for the growing season. It performed well during the dry season though. This issue with MODIS GPP in dry water limited environments, both in the Sahel and in other locations, has been observed by other studies such as (Leuning et al. 2005;

Heinsch et al. 2006; Kanniah et al. 2009; Sjöström et al. 2011; Sjöström et al. 2013).

2. *How does the GPP calculated from MSG/SEVIRI for the Sahel compare to the MODIS GPP product?*

The GPP derived from the two sensors are different. GPP calculated from MSG/SEVIRI data showed, due to its high temporal resolution, strong day-to-day variability. MODIS GPP on the other hand has lower temporal resolution and did not capture any short term variation in GPP. Seasonality was captured by both products, though the actual GPP values were much higher for MSG/SEVIRI during the growing season. The size of the data used was much higher for MSG/SEVIRI compared to MODIS data. For the study period the raw data files from MSG/SEVIRI was 35.3 GB of data. For MODIS on the other hand it was 766 MB for the same time period. If storage and processing power is a concern, this might cause problems. Especially if the study involves time series longer than a few years. The additional data also means that more processing power is needed to compute GPP quickly.

3. *If the products provide different results, what might be the best use for each of them?* **(***This of course depends on what questions are being asked.)*

MSG/SEVIRI derived GPP provides a higher temporal resolution and more accurate GPP estimation, which could be improved with a more accurate LUE model. Therefore it would be more accurate to use in studies where actual magnitude of GPP is important, for example carbon budgets, yield estimation and vegetation productivity. Early warning systems trying to predict food security with remote sensing, such as Oroda (2002) could benefit from the more accurate GPP estimation of MSG/SEVIRI. Supply and demand studies of NPP such as Abdi et al. (2014) could also benefit from more accurate GPP, from which NPP can be derived. If 41% of NPP is consumed by humans (Abdi et al. 2014) underestimating NPP, or GPP, can have a large effect on the result.

MODIS GPP performs well during the dry season, which is of little importance, and captures seasonality well. Its main problem is the underestimation of GPP during the growing season. MODIS would be suitable for use when the actual magnitudes of GPP is not as important as more general trends and patterns. Then the underestimation is less important. MODIS GPP is also suitable for long time series. Both due to the fact that the MODIS GPP is available for more years than relevant MSG/SEVIRI data and due to the smaller file sizes which makes storage and processing less of a problem.

5 CONCLUSIONS

The study concludes that MSG/SEVIRI derived GPP performs better than MODIS GPP in the Sahel for 2011-2012 with respect to accuracy of the estimated GPP values when compared to *in situ* EC GPP, and also in capturing the day-to-day variance. However, this variance does not always accurately represent the EC GPP variance.

MSG/SEVIRI GPP should therefore be more suitable when studying carbon budgets, yield estimation and vegetation productivity. MODIS GPP should be more suitable when studying more general trends and patterns in GPP. If data storage and processing power is a concern MODIS data is much less demanding than MSG/SEVIRI data.

6 REFERENCES

Abdi, H., J. Seaquist, D. Tenenbaum, L. Eklundh, and J. Ardö. 2014. The supply and demand of net primary production in the Sahel. *Environmental Research Letters,* 9**:** 1-11.

Ahlström, A., M. R. Raupach, G. Schurgers, B. Smith, A. Arneth, M. Jung, M. Reichstein, J. G. Canadell, et al. 2015. The dominant role of semi-arid ecosystems in the trend and variability of the land CO2 sink. *Science,* 348**:** 895-899. DOI: 10.1126/science.aaa1668

Aminou, D. M. A. 2002. MSG's SEVIRI instrument. *ESA Bull.,* 111.

Ardö, J., M. Mölder, B. A. El-Tahir, and H. A. Elkhidir. 2008. Seasonal variation of carbon fluxes in a sparse savanna in semi arid Sudan. *Carbon Balance and Management,* 3.

Asrar, G., R. B. Myneni, and B. J. Choudhury. 1992. Spatial heterogeneity in vegetation canopies and remote sensing of absorbed photosynthetically active radiation: A modeling study. *Remote Sensing of Environment,* 41**:** 85-103. DOI: http://dx.doi.org/10.1016/0034-4257(92)90070-Z

Bader, J., and M. Latif. 2003. The impact of decadal-scale Indian Ocean sea surface temperature anomalies on Sahelian rainfall and the North Atlantic Oscillation. *Geophysical Research Letters,* 30.

Batterbury, S., and A. Warren. 2001. The African Sahel 25 years after the great drought: assessing progress and moving towards new agendas and approaches. *Global Environmental Change,* 11**:** 1-8. DOI: http://dx.doi.org/10.1016/S0959-3780(00)00040-6

Beer, C., M. Reichstein, E. Tomelleri, P. Ciais, M. Jung, N. Carvalhais, C. Rödenbeck, M. A. Arain, et al. 2010. Terrestrial gross carbon dioxide uptake: global distribution and covariation with climate. *Science,* 329**:** 834-838.

Belward, A. S. 1996. *The IGBP-DIS Global 1 Km Land Cover Data Set "DISCover": Proposal and Implementation Plans: Report of the Land Recover Working Group of IGBP-DIS*. IGBP-DIS.

Brandt, M., C. Mbow, A. A. Diouf, A. Verger, C. Samimi, and R. Fensholt. 2015. Ground-and satellite-based evidence of the biophysical mechanisms behind the greening Sahel. *Global change biology*.

Breman, H., J. R. Groot, and H. van Keulen. 2001. Resource limitations in Sahelian agriculture. *Global Environmental Change,* 11**:** 59-68.

Brisson, A., P. Le Borgne, and A. Marsouin. 1999. Development of algorithms for surface solar irradiance retrieval at O&SI SAF low and mid latitudes. *Eumetsat Ocean and Sea Ice SAF internal project team report*.

Chapin, F. S., P. A. Matson, and H. A. Mooney. 2002. *Principles of Terrestrial Ecosystem Ecology*.

Coops, N. C., T. A. Black, R. S. Jassal, J. A. Trofymow, and K. Morgenstern. 2007. Comparison of MODIS, eddy covariance determined and physiologically modelled gross primary production (GPP) in a Douglas-fir forest stand. *Remote Sensing of Environment,* 107**:** 385-401. DOI: http://dx.doi.org/10.1016/j.rse.2006.09.010

Dardel, C., L. Kergoat, P. Hiernaux, E. Mougin, M. Grippa, and C. J. Tucker. 2014. Re-greening Sahel: 30 years of remote sensing data and field observations (Mali, Niger). *Remote Sensing of Environment,* 140**:** 350-364. DOI: http://dx.doi.org/10.1016/j.rse.2013.09.011

Donohue, R., I. Hume, M. Roderick, T. McVicar, J. Beringer, L. Hutley, J. Gallant, J. Austin, et al. 2014. Evaluation of the remote-sensing-based DIFFUSE model for estimating photosynthesis of vegetation. *Remote Sensing of Environment*, 155**:** 349-365.

Drolet, G. G., E. M. Middleton, K. F. Huemmrich, F. G. Hall, B. D. Amiro, A. G. Barr, T. A. Black, J. H. McCaughey, et al. 2008. Regional mapping of gross light-use efficiency using MODIS spectral indices. *Remote Sensing of Environment*, 112**:** 3064-3078. DOI: http://dx.doi.org/10.1016/j.rse.2008.03.002

ESA. 2015. http://www.esa.int/Our_Activities/Observing_the_Earth/Meteosat_Second_Generation/MSG_overview2. Retrieved April 21 2015, from

Falge, E., D. Baldocchi, J. Tenhunen, M. Aubinet, P. Bakwin, P. Berbigier, C. Bernhofer, G. Burba, et al. 2002. Seasonality of ecosystem respiration and gross primary production as derived from FLUXNET measurements. *Agricultural and Forest Meteorology*, 113**:** 53-74. DOI: http://dx.doi.org/10.1016/S0168-1923(02)00102-8

Fensholt, R., I. Sandholt, M. S. Rasmussen, S. Stisen, and A. Diouf. 2006. Evaluation of satellite based primary production modelling in the semi-arid Sahel. *Remote Sensing of Environment*, 105**:** 173-188.

Folland, C., T. Palmer, and D. Parker. 1986. Sahel rainfall and worldwide sea temperatures, 1901–85. *Nature*, 320**:** 602-607.

Frouin, R., D. W. Lingner, C. Gautier, K. S. Baker, and R. C. Smith. 1989. A simple analytical formula to compute clear sky total and photosynthetically available solar irradiance at the ocean surface. *Journal of Geophysical Research: Oceans (1978–2012)*, 94**:** 9731-9742.

Frouin, R., and R. T. Pinker. 1995. Estimating Photosynthetically Active Radiation (PAR) at the earth's surface from satellite observations. *Remote Sensing of Environment*, 51**:** 98-107. DOI: http://dx.doi.org/10.1016/0034-4257(94)00068-X

Garbulsky, M. F., J. Peñuelas, D. Papale, J. Ardö, M. L. Goulden, G. Kiely, A. D. Richardson, E. Rotenberg, et al. 2010. Patterns and controls of the variability of radiation use efficiency and primary productivity across terrestrial ecosystems. *Global Ecology and Biogeography*, 19**:** 253-267.

Gautier, C., G. Diak, and S. Masse. 1980. A simple physical model to estimate incident solar radiation at the surface from GOES satellite data. *Journal of Applied Meteorology*, 19**:** 1005-1012.

GCOS, 2003. Summary Report of the eleventh session of the WMO-IOC-UNEP-ICSU (WMO/TD-No.1189). Report, Melbourne, Australia. [in Swedish, English summary]

Geiger, B., D. Carrer, L. Franchisteguy, J.-L. Roujean, and C. Meurey. 2008. Land surface albedo derived on a daily basis from Meteosat second generation observations. *Geoscience and Remote Sensing, IEEE Transactions on*, 46**:** 3841-3856.

Gilabert, M. A., A. Moreno, F. Maselli, B. Martínez, M. Chiesi, S. Sánchez-Ruiz, F. J. García-Haro, A. Pérez-Hoyos, et al. 2015. Daily GPP estimates in Mediterranean ecosystems by combining remote sensing and meteorological data. *ISPRS Journal of Photogrammetry and Remote Sensing*, 102**:** 184-197. DOI:

http://dx.doi.org/10.1016/j.isprsjprs.2015.01.017

Gobron, N., and M. M. Verstraete, 2009. FAPAR. Global Terrestrial Observing System, Report, Rome. [in Swedish, English summary]

Goetz, S., and S. D. Prince. 1999. Modelling terrestrial carbon exchange and storage: evidence and implications of functional convergence in light-use efficiency. *Advances in ecological research*, 28**:** 57-92.

Hanan, N. P., P. Kabat, A. J. Dolman, and J. Elbers. 1998. Photosynthesis and carbon balance of a Sahelian fallow savanna. *Global change biology*, 4**:** 523-538.

Heinsch, F. A., M. Reeves, P. Votava, S. Kang, C. Milesi, M. Zhao, J. Glassy, W. M. Jolly, et al. 2003. GPP and NPP (MOD17A2/A3) Products NASA MODIS Land Algorithm. *MOD17 User's Guide***:** 1-57.

Heinsch, F. A., M. Zhao, S. W. Running, J. S. Kimball, R. R. Nemani, K. J. Davis, P. V. Bolstad, B. D. Cook, et al. 2006. Evaluation of remote sensing based terrestrial productivity from MODIS using regional tower eddy flux network observations. *Geoscience and Remote Sensing, IEEE Transactions on*, 44**:** 1908-1925.

Herrmann, S. M., A. Anyamba, and C. J. Tucker. 2005. Recent trends in vegetation dynamics in the African Sahel and their relationship to climate. *Global Environmental Change*, 15**:** 394-404. DOI: http://dx.doi.org/10.1016/j.gloenvcha.2005.08.004

Hickler, T., L. Eklundh, J. W. Seaquist, B. Smith, J. Ardö, L. Olsson, M. T. Sykes, and M. Sjöström. 2005. Precipitation controls Sahel greening trend. *Geophysical Research Letters*, 32.

Iqbal, M. 1983. *An introduction to solar radiation*. Orlando: Academic Press.

Kanniah, K., J. Beringer, L. Hutley, N. Tapper, and X. Zhu. 2009. Evaluation of Collections 4 and 5 of the MODIS Gross Primary Productivity product and algorithm improvement at a tropical savanna site in northern Australia. *Remote Sensing of Environment*, 113**:** 1808-1822.

Leuning, R., H. A. Cleugh, S. J. Zegelin, and D. Hughes. 2005. Carbon and water fluxes over a temperate Eucalyptus forest and a tropical wet/dry savanna in Australia: measurements and comparison with MODIS remote sensing estimates. *Agricultural and Forest Meteorology*, 129**:** 151-173.

Lillesand, T. M., R. W. Kiefer, and J. W. Chipman. 2008. *Remote Sensing and Image Interpretation*. Wiley

LSA-SAF. 2008. Validation report Vegetation Parameters (FVC, LAI, FAPAR). *Ref: SAF/LAND/UV/VR_VEGA/2.1*.

LSA-SAF. 2011a. Product user manual Down-welling Surface Shortwave Flux (DSSF). *Ref: SAF/LAND/MF/PUM_DSSF/2.6v2*.

LSA-SAF. 2011b. Validation report Down-welling Surface Shortwave Flux (DSSF). *Ref: SAF/LAND/MF/VR_DSSF/I_11v4*.

LSA-SAF. 2013. Product user manual Vegetation Parameters (VEGA). *Ref: SAF/LAND/UV/PUM_VEGA/2.1-4*.

Lucio, P., L. Molion, F. Conde, and M. de Melo. 2012. A study on the west Sahel rainfall variability: The role of the intertropical convergence zone (ITCZ). *African Journal of Agricultural Research*, 7**:** 2096-2013.

Martínez, B., F. Camacho, A. Verger, F. J. García-Haro, and M. A. Gilabert. 2013. Intercomparison and quality

assessment of MERIS, MODIS and SEVIRI FAPAR products over the Iberian Peninsula. *International Journal of Applied Earth Observation and Geoinformation,* 21**:** 463-476. DOI: http://dx.doi.org/10.1016/j.jag.2012.06.010

Martínez, B., A. Moreno, S. Sánchez, F. J. Garcia-Haro, F. Camacho, J. Meliá, J. Ardö, W. Kutsch, et al. 2015. Mapping daily gross primary production over Africa using SEVIRI/MSG satellite products. UNPUBLISHED.

McCree, K. J. 1981. Photosynthetically Active Radiation. In *Physiological Plant Ecology I,* eds. O. L. Lange, P. S. Nobel, C. B. Osmond, and H. Ziegler, 41-55. Springer Berlin Heidelberg.

Mertz, O., C. Mbow, A. Reenberg, and A. Diouf. 2009. Farmers' perceptions of climate change and agricultural adaptation strategies in rural Sahel. *Environmental Management,* 43**:** 804-816.

Monteith, J. L. 1972. Solar Radiation and Productivity in Tropical Ecosystems. *Journal of Applied Ecology*, 9**:** 747-766. DOI: 10.2307/2401901

Moreno, A., F. Maselli, M. A. Gilabert, M. Chiesi, B. Martínez, and G. Seufert. 2012. Assessment of MODIS imagery to track light-use efficiency in a water-limited Mediterranean pine forest. *Remote Sensing of Environment,* 123**:** 359-367. DOI: http://dx.doi.org/10.1016/j.rse.2012.04.003

Myneni, R. B., S. O. Los, and G. Asrar. 1995. Potential gross primary productivity of terrestrial vegetation from 1982–1990. *Geophysical Research Letters*, 22**:** 2617-2620. DOI: 10.1029/95GL02562

Nemani, R. R., C. D. Keeling, H. Hashimoto, W. M. Jolly, S. C. Piper, C. J. Tucker, R. B. Myneni, and S. W. Running. 2003. Climate-driven increases in global terrestrial net primary production from 1982 to 1999. *science,* 300**:** 1560-1563.

Niang, I., O. C. Ruppel, M. A. Abdrabo, A. Essel, C. Lennard, J. Padgham, and P. Urquhart. 2014. Africa. In *Climate Change 2014: Impacts, Adaptation, and Vulnerability. Part B: Regional Aspects. Contribution of Working Group II to the Fifth Assessment Report of the Intergovernmental Panel of Climate Change,* eds. V. R. Barros, C. B. Field, D. J. Dokken, M. D. Mastrandrea, K. J. Mach, T. E. Bilir, M. Chatterjee, K. L. Ebi, Y. O. Estrada, R. C. Genova, B. Girma, E. S. Kissel, A. N. Levy, S. MacCracken, P. R. Mastrandrea, and L. L. White, 1199-1265. Cambridge, United Kingdom and New York, NY, USA: Cambridge University Press.

Nicholson, S. E. 1981. Rainfall and Atmospheric Circulation during Drought Periods and Wetter Years in West Africa. *Monthly Weather Review,* 109**:** 2191-2208. DOI: 10.1175/1520-0493(1981)109<2191:RAACDD>2.0.CO;2

Nicholson, S. E., and J. Kim. 1997. The relationship of the El Nino-Southern oscillation to African rainfall. *International Journal of Climatology,* 17**:** 117-135.

Olsson, L., L. Eklundh, and J. Ardö. 2005. A recent greening of the Sahel—trends, patterns and potential causes. *Journal of Arid Environments,* 63**:** 556-566. DOI: http://dx.doi.org/10.1016/j.jaridenv.2005.03.008

Oroda, A. 2002. Application of remote sensing to early warning for food security and environmental monitoring in the horn of Africa. *INTERNATIONAL ARCHIVES OF*

PHOTOGRAMMETRY AND REMOTE SENSING, 34**:** 66-72.

Plummer, S. 2006. On validation of the MODIS gross primary production product. *Geoscience and Remote Sensing, IEEE Transactions on*, 44**:** 1936-1938. DOI: 10.1109/TGRS.2006.872521

Poulter, B., D. Frank, P. Ciais, R. B. Myneni, N. Andela, J. Bi, G. Broquet, J. G. Canadell, et al. 2014. Contribution of semi-arid ecosystems to interannual variability of the global carbon cycle. *Nature*, 509**:** 600-603.

Roehrig, R., D. Bouniol, F. Guichard, F. Hourdin, and J.-L. Redelsperger. 2013. The present and future of the West African monsoon: a process-oriented assessment of CMIP5 simulations along the AMMA transect. *Journal of Climate*, 26**:** 6471-6505.

Rogerson, P. A. 2010. Statistical methods for geography. In *Statistical methods for geography*. Los Angeles | London | New Dehli | Singapore | Washington DC: SAGE Publications Ltd.

Running, S., P. Thornton, R. Nemani, and J. Glassy. 2000. Global Terrestrial Gross and Net Primary Productivity from the Earth Observing System. In *Methods in Ecosystem Science*, eds. O. Sala, R. Jackson, H. Mooney, and R. Howarth, 44-57. Springer New York.

Running, S. W., R. Nemani, J. M. Glassy, and P. E. Thornton. 1999. MODIS daily photosynthesis (PSN) and annual net primary production (NPP) product (MOD17): Algorithm Theoretical Basis Document. *University of Montana, SCF At-Launch Algorithm ATBD Documents (available online at: www. ntsg. umt. edu/modis/ATBD/ATBD_MOD17_v 21. pdf)*.

Running, S. W., R. R. Nemani, F. A. Heinsch, M. Zhao, M. Reeves, and H. Hashimoto. 2004. A Continuous Satellite-Derived Measure of Global Terrestrial Primary Production. *BioScience*, 54**:** 547-560. DOI: 10.1641/0006-3568(2004)054[0547:acsmog]2.0.co;2

Ryan, M. G. 1991. Effects of climate change on plant respiration. *Ecological Applications*, 1**:** 157-167.

Seaquist, J., T. Hickler, L. Eklundh, J. Ardö, and B. Heumann. 2009. Disentangling the effects of climate and people on Sahel vegetation dynamics. *Biogeosciences*, 6**:** 469-477.

Sitch, S., B. Smith, I. C. Prentice, A. Arneth, A. Bondeau, W. Cramer, J. Kaplan, S. Levis, et al. 2003. Evaluation of ecosystem dynamics, plant geography and terrestrial carbon cycling in the LPJ dynamic global vegetation model. *Global Change Biology*, 9**:** 161-185.

Sjöström, M., J. Ardö, A. Arneth, N. Boulain, B. Cappelaere, L. Eklundh, A. de Grandcourt, W. L. Kutsch, et al. 2011. Exploring the potential of MODIS EVI for modeling gross primary production across African ecosystems. *Remote Sensing of Environment*, 115**:** 1081-1089. DOI: http://dx.doi.org/10.1016/j.rse.2010.12.013

Sjöström, M., M. Zhao, S. Archibald, A. Arneth, B. Cappelaere, U. Falk, A. De Grandcourt, N. Hanan, et al. 2013. Evaluation of MODIS gross primary productivity for Africa using eddy covariance data. *Remote sensing of environment*, 131**:** 275-286.

Sultan, B., and S. Janicot. 2000. Abrupt shift of the ITCZ over West Africa and intra-seasonal variability. *Geophysical Research Letters*, 27**:**

3353-3356. DOI: 10.1029/1999GL011285

Tagesson, T., R. Fensholt, F. Cropley, I. Guiro, S. Horion, A. Ehammer, and J. Ardö. 2015a. Dynamics in carbon exchange fluxes for a grazed semi-arid savanna ecosystem in West Africa. *Agriculture, Ecosystems & Environment*, 205**:** 15-24.

Tagesson, T., R. Fensholt, I. Guiro, M. O. Rasmussen, S. Huber, C. Mbow, M. Garcia, S. Horion, et al. 2015b. Ecosystem properties of semiarid savanna grassland in West Africa and its relationship with environmental variability. *Global change biology*, 21**:** 250-264.

Traore, A. K., P. Ciais, N. Vuichard, N. MacBean, C. Dardel, B. Poulter, S. Piao, J. B. Fisher, et al. 2014. 1982–2010 Trends of light use efficiency and inherent water use efficiency in African vegetation: sensitivity to climate and atmospheric CO2 concentrations. *Remote Sensing*, 6**:** 8923-8944.

Turner, D. P., W. D. Ritts, W. B. Cohen, S. T. Gower, S. W. Running, M. Zhao, M. H. Costa, A. A. Kirschbaum, et al. 2006. Evaluation of MODIS NPP and GPP products across multiple biomes. *Remote Sensing of Environment*, 102**:** 282-292. DOI: http://dx.doi.org/10.1016/j.rse.2006.02.017

Wang, G., and E. A. B. Eltahir. 2000. Ecosystem dynamics and the Sahel Drought. *Geophysical Research Letters*, 27**:** 795-798. DOI: 10.1029/1999GL011089

Waring, H. R., and S. W. Running. 2007. *Forest Ecosystems: Analysis at Multiple Scales*. San Diego: Academic Press.

Zhang, F., J. M. Chen, J. Chen, C. M. Gough, T. A. Martin, and D. Dragoni. 2012. Evaluating spatial and temporal patterns of MODIS GPP over the conterminous U.S. against flux measurements and a process model. *Remote Sensing of Environment*, 124**:** 717-729. DOI: http://dx.doi.org/10.1016/j.rse.2012.06.023

Zhang, Y., G. Yu, J. Yang, M. C. Wimberly, X. Zhang, J. Tao, Y. Jiang, and J. Zhu. 2014. Climate-driven global changes in carbon use efficiency. *Global Ecology and Biogeography*, 23**:** 144-155. DOI: 10.1111/geb.12086

Zhao, M., and S. W. Running. 2010. Drought-induced reduction in global terrestrial net primary production from 2000 through 2009. *science*, 329**:** 940-943.

7 APPENDIX

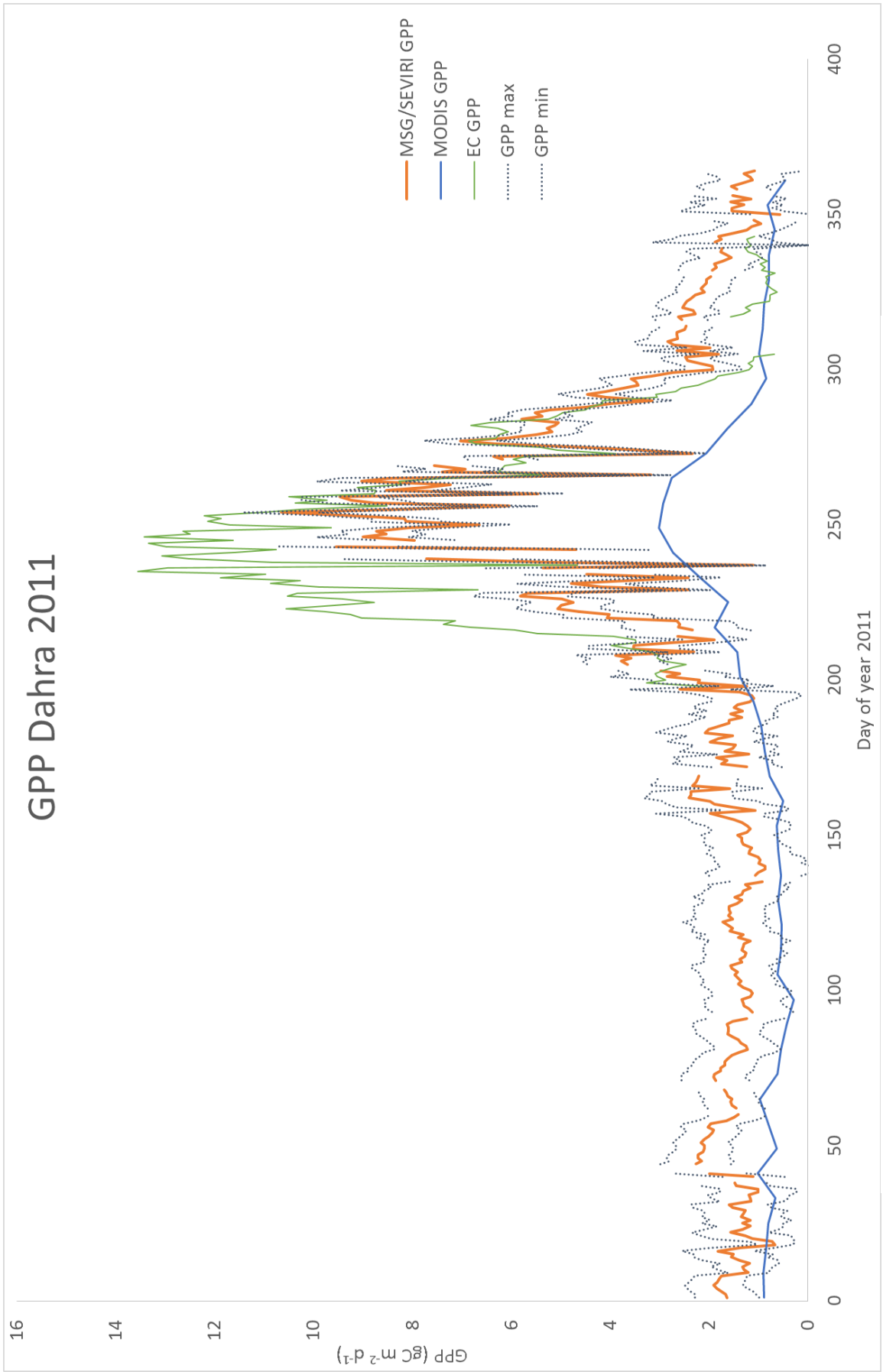

Figure A1: GPP in Dahra for 2011 from MSG/SEVIRI, MODIS and in situ *measurements. The dotted lines are GPP uncertainties due to theoretical errors in the MSG/SEVIRI FAPAR product.*

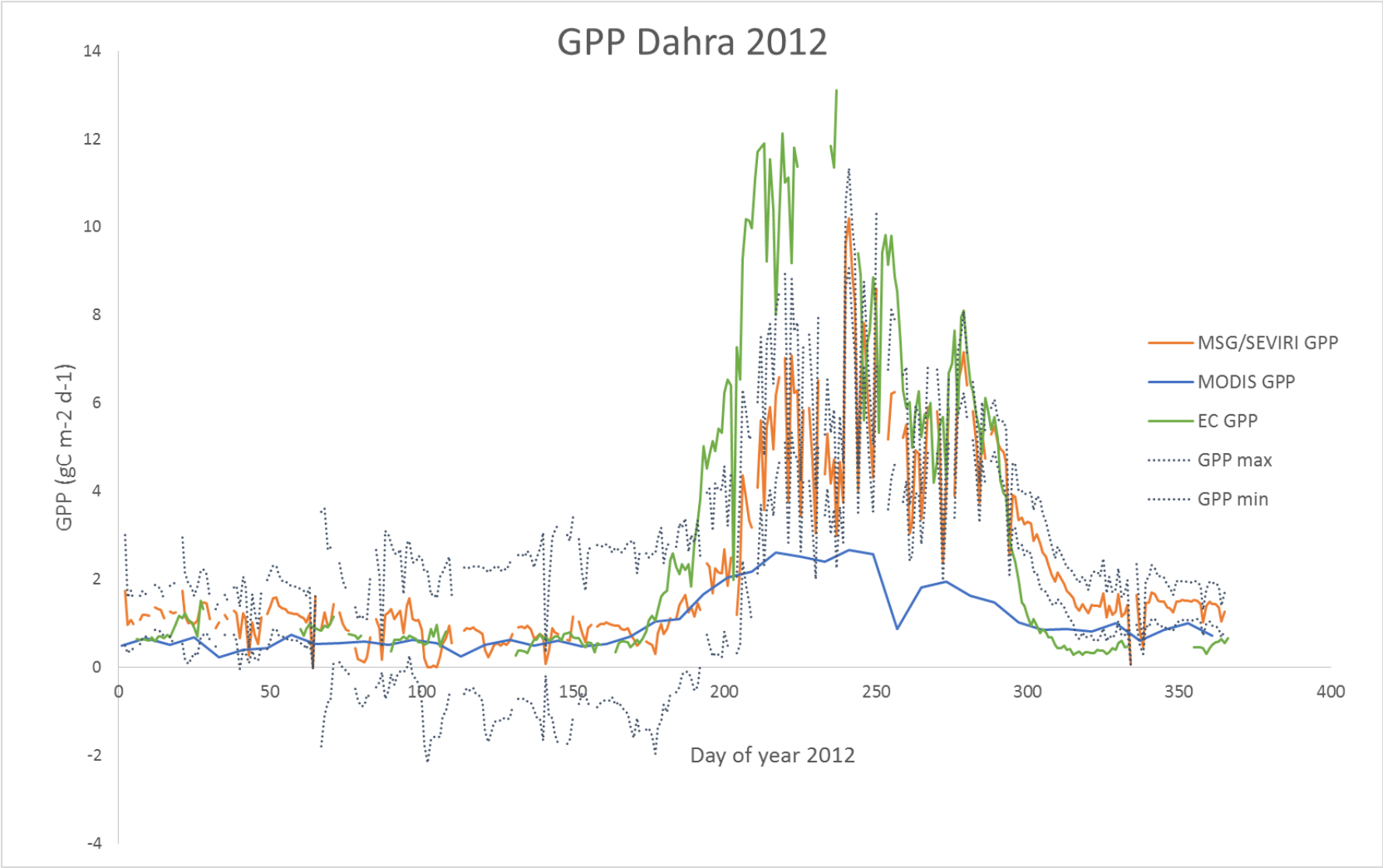

Figure A2: GPP in Dahra for 2012 from MSG/SEVIRI, MODIS and in situ *measurements. The dotted lines are GPP uncertainties due to theoretical errors in the MSG/SEVIRI FAPAR product.*

Institutionen för naturgeografi och ekosystemvetenskap, Lunds Universitet.

Student examensarbete (Seminarieuppsatser). Uppsatserna finns tillgängliga på institutionens geobibliotek, Sölvegatan 12, 223 62 LUND. Serien startade 1985. Hela listan och själva uppsatserna är även tillgängliga på LUP student papers (www.nateko.lu.se/masterthesis) och via Geobiblioteket (www.geobib.lu.se)

The student thesis reports are available at the Geo-Library, Department of Physical Geography and Ecosystem Science, University of Lund, Sölvegatan 12, S-223 62 Lund, Sweden. Report series started 1985. The complete list and electronic versions are also electronic available at the LUP student papers (www.nateko.lu.se/masterthesis) and through the Geo-library (www.geobib.lu.se)

315 Emelie Norhagen (2014) Växters fenologiska svar på ett förändrat klimat - modellering av knoppsprickning för hägg, björk och asp i Skåne

316 Liisi Nõgu (2014) The effects of site preparation on carbon fluxes at two clear-cuts in southern Sweden

317 Julian Will (2014) Development of an automated matching algorithm to assess the quality of the OpenStreetMap road network - A case study in Göteborg, Sweden

318 Niklas Olén (2011) Water drainage from a Swedish waste treatment facility and the expected effect of climate change

319 Wösel Thoresen (2014) Burn the forest - Let it live. Identifying potential areas for controlled forest fires on Gotland using Geographic Information System

320 Jurgen van Tiggelen (2014) Assimilation of satellite data and in-situ data for the improvement of global radiation maps in the Netherlands.

321 Sam Khallaghi (2014) Posidonia Oceanica habitat mapping in shallow coastal waters along Losinj Island, Croatia using Geoeye-1 multispectral imagery.

322 Patrizia Vollmar (2014) The influence of climate and land cover on wildfire patterns in the conterminous United States

323 Marco Giljum (2014) Object-Based Classification of Vegetation at Stordalen Mire near Abisko by using High-Resolution Aerial Imagery

324 Marit Aalrust Ripel (2014) Natural hazards and farmers experience of climate change on highly populated Mount Elgon, Uganda

325 Benjamin Kayatz (2014) Modelling of nitrous oxide emissions from clover grass ley – wheat crop rotations in central eastern Germany - An application of DNDC

326 Maxime Rwaka (2014) An attempt to investigate the impact of 1994 Tutsi Genocide in Rwanda on Landscape using Remote Sensing and GIS analysis

327 Ruibin Xu (2014) Spatial analysis for the distribution of cells in tissue sections

328 Annabelle Finck (2014) Bird biodiversity in relation to forest composition in Sweden

329 Tetiana Svystun (2015) Modeling the potential impact of climate change on the distribution of Western Corn Rootworm in Europe”

330 Joel Forsmoo (2014) The European Corn Borer in Sweden: A Future Perspective Based on a Phenological Model Approach

331 Andrew Ekoka Mwambo (2015) Estimation of Cropland Ecological

Footprint within Danish Climate Commissions 2050 Scenarios for Land use and Bioenergy Consumption

332 Anna Lindstein (2015) Land-atmosphere exchange of carbon dioxide in a high Arctic fen: importance of wintertime fluxes

333 Karla Susana Markley Vergara (2015) Present and near future water availability for closing yield gaps in four crops in South America

334 Klara Århem & Fredrik Fredén (2015) Land cover change and its influence on soil erosion in the Mara region, Tanzania: Using satellite remote sensing and the Revised Universal Soil Loss Equation (RUSLE) to map land degradation between 1986 and 2013

335 Fei Lu (2015) Compute a Crowdedness Index on Historical GIS Data- A Case Study of Hög Parish, Sweden, 1812-1920

336 Lina Allesson (2015) Impact of photo-chemical processing of dissolved organic carbon on the bacterial respiratory quotient in aquatic ecosystems

337 Andreas Kiik (2015) Cartographic design of thematic polygons: a comparison using eye-movement metrics analysis

338 Iain Lednor (2015) Testing the robustness of the Plant Phenology Index to changes in temperature

339 Louise Bradshaw (2015) Submerged Landscapes - Locating Mesolithic settlements in Blekinge, Sweden

340 Elisabeth Maria Farrington (2015) The water crisis in Gaborone: Investigating the underlying factors resulting in the 'failure' of the Gaborone Dam, Botswana

341 Annie Forssblad (2015) Utvärdering av miljöersättning för odlingslandskapets värdefulla träd

342 Iris Behrens, Linn Gardell (2015) Water quality in Apac-, Mbale- & Lira district, Uganda - A field study evaluating problems and suitable solutions

343 Linnéa Larsson (2015) Analys av framtida översvämningsrisker i Malmö - En fallstudie av Castellums fastigheter

344 Ida Pettersson (2015) Comparing Ips Typographus and Dendroctonus ponderosas response to climate change with the use of phenology models

345 Frida Ulfves (2015) Classifying and Localizing Areas of Forest at Risk of Storm Damage in Kronoberg County

346 Alexander Nordström (2015) Förslag på dammar och skyddsområde med hjälp av GIS: En studie om löv- och klockgroda i Ystad kommun, Skåne

347 Samanah Seyedi-Shandiz (2015) Automatic Creation of Schematic Maps - A Case Study of the Railway Network at the Swedish Transport Administration

348 Johanna Andersson (2015) Heat Waves and their Impacts on Outdoor Workers – A Case Study in Northern and Eastern Uganda

349 Jimmie Carpman (2015) Spatially varying parameters in observed new particle formation events

350 Mihaela – Mariana Tudoran (2015) Occurrences of insect outbreaks in Sweden in relation to climatic parameters since 1850

351 Maria Gatzouras (2015) Assessment of trampling impact in Icelandic natural areas in experimental plots with focus on image analysis of digital photographs

352 Gustav Wallner (2015) Estimating and evaluating GPP in the Sahel using MSG/SEVIRI and MODIS satellite data